Rao. *Vessel Plus* 2022;6:26
DOI: 10.20517/2574-1209.2021.93

Vessel Plus

Review

Open Access

Echocardiography: an overview - Part III

P. Syamasundar Rao

Children's Heart Institute, University of Texas at Houston, McGovern Medical School and Children's Memorial Hermann Hospital, Houston, TX 77030, USA.

Correspondence to: P. Syamasundar Rao, MD, University of Texas at Houston, McGovern Medical School, 6410 Fannin Street, Suite #425, Houston, TX 77030, USA. E-mail: P.Syamasundar.Rao@uth.tmc.edu

How to cite this article: Rao PS. Echocardiography: an overview - Part III. *Vessel Plus* 2022;6:26. https://dx.doi.org/10.20517/2574-1209.2021.93

Received: 1 Jul 2021 **First Decision:** 20 Jan 2022 **Revised:** 27 Jan 2022 **Accepted:** 1 Mar 2022 **Published:** 29 Apr 2022

Academic Editor: Frank W. Sellke **Copy Editor:** Xi-Jun Chen **Production Editor:** Xi-Jun Chen

Abstract

This review describes echocardiographic features of commonly encountered cyanotic congenital heart defects. Echo-Doppler characteristics of more commonly seen defects: tetralogy of Fallot, transposition of the great arteries, tricuspid atresia, total anomalous pulmonary venous connection, and truncus arteriosus were first discussed. Then, hypoplastic left heart syndrome followed by less commonly observed lesions such as double-outlet right ventricle, double-inlet left ventricle, interrupted aortic arch, pulmonary atresia with an intact ventricular septum, congenitally corrected transposition of the great arteries, Ebstein's anomaly of the tricuspid valve, and mitral atresia with normal aortic root were reviewed.

Keywords: Echocardiography, Doppler, tetralogy of Fallot, transposition of the great arteries, tricuspid atresia, total anomalous pulmonary venous connection, truncus arteriosus, hypoplastic left heart syndrome

INTRODUCTION

In Part I of this review, principles of echo-Doppler studies, the methods of recording echocardiographic studies, methods of appraisal of pressures in the pulmonary artery (PA), assessment of left, right and single ventricular systolic function, and illustration of the usefulness of echo studies in evaluating multiple neonatal issues were described. In Part II, echocardiographic features of commonly seen acyanotic heart defects were reviewed. In this Part III, I will present a succinct review of echocardiographic findings of cyanotic congenital heart defects (CHDs). A concise portrayal of each defect's pathology and altered physiology will be presented first, followed by the echocardiographic findings. Most cyanotic CHDs are

© The Author(s) 2022. **Open Access** This article is licensed under a Creative Commons Attribution 4.0 International License (https://creativecommons.org/licenses/by/4.0/), which permits unrestricted use, sharing, adaptation, distribution and reproduction in any medium or format, for any purpose, even commercially, as long as you give appropriate credit to the original author(s) and the source, provide a link to the Creative Commons license, and indicate if changes were made.

usually identified during prenatal echo studies, as reviewed elsewhere[1,2]; in this review, only post-natal findings are reviewed.

TETRALOGY OF FALLOT

Tetralogy of Fallot (TOF) is the utmost frequent cyanotic CHD in patients who are more than one year of age. The defect comprises 10% of all heart defects[3-6]. TOF is a constellation of four abnormalities, namely, (1) ventricular septal defect; (2) pulmonary stenosis; (3) hypertrophy of the right ventricle (RV); and (4) dextroposition of the aorta[3-6]. The ventricular septal defects (VSDs) typically abut directly on the atrioventricular component of the membranous septum and are called as perimembranous VSDs and are large and non-restrictive. At times the VSD encompasses the muscular portion of the ventricular septum. Rarely, other defects in the muscular septum may coexist. Pulmonary stenosis (PS) varies both in regard to the location of the narrowing and the magnitude of obstruction. The extent of narrowing may be noticeably mild, not producing any decrease in arterial O_2 saturation. Indeed, left to right shunting via the VSD may occur. Or, the obstruction may be substantial, causing marked cyanosis even in the neonate. The location of the narrowing may be situated in the infundibular region, at the valve itself, in a supra-valvar site, or at the branch PAs; infundibular narrowing is the most common obstructive lesion among these. The narrowing may be located at one of the above sites or may involve several locations. The infundibular narrowing in TOF is considered to be caused by superior and anterior deviation of the conal (infundibular) ventricular septum. The valve narrowing may be due to fusion of pulmonary valve commissures, hypoplasia of the annulus of the pulmonary valve, or a mixture of the two. Sometimes, pulmonary valve leaflet dysplasia may be present, causing the obstruction. Hypertrophy of the RV is seen in all patients and is generally severe in degree. Aortic over-ride of the ventricular septum and rightward displacement (dextroposition) of the aorta varies from one patient to the other. Dilatation of the aorta is seen, which is secondary to an abnormality of development instead of the pathophysiology of tetralogy. The right-sided descending aorta is seen in 25% to 30% of tetralogy patients[5,7,8]. Atrial septal defects (ASDs) of significant size may be seen in some TOF patients; in such instances, the condition is called pentalogy of Fallot. In one study, ASDs were seen in 27% of autopsy specimens[8].

Because the ventricular defect is large and non-restrictive, the pressures in both ventricles are equal, and both right and left ventricles function as a single unit. The relative quantities of blood flowing into the pulmonary and systemic circulations depend on the resistances offered by the systemic circuit (systemic vascular resistance) *vs.* degree of RV outflow tract narrowing. The greater the RV outflow obstruction, the lesser is the blood flow into the lung. In a typical tetralogy patient, the resistance presented by the RV outflow tract stenosis is greater than that of the systemic vascular resistance; consequently, right to left shunt takes place through the ventricular defect.

Several types of TOF exist and each type has its own mode of presentation. Furthermore, the type of management differs from one type to the other[5,6]. On the basis of these considerations, we recommend the following classification[5,6]: (1) Type I, classic TOF; (2) Type II, TOF with pulmonary atresia; (3) Type III, TOF with multiple aorto-pulmonary collateral arteries (MAPCAs); and (4) Type IV, TOF with the syndrome of absent pulmonary valve. The echo features of the different types are reviewed one after the other.

Type I, classic TOF

An echocardiographic examination is valuable in establishing the diagnosis. A large VSD is clearly imaged along with an over-riding of the aorta [Figure 1]. A dilated and hypertrophied RV is seen. Usually, there is a right to left shunt through the VSD [Figure 2] and this, along with RV outflow tract stenosis [Figure 3] can

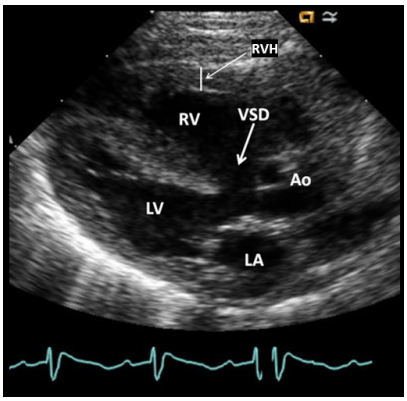

Figure 1. Selected video frame from a 2D echocardiogram in a parasternal long-axis view of a patient with tetralogy of Fallot demonstrates a large ventricular septal defect (VSD) (thick arrow) and an over-riding aorta (Ao). The right ventricle (RV) is enlarged and hypertrophied (RVH) (thin arrow). Reproduced from Ref.[5]. LA: Left atrium; LV: left ventricle.

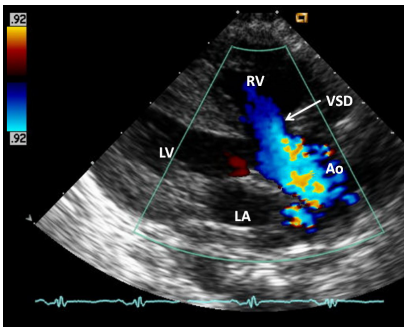

Figure 2. Color Doppler flow mapping of a similar echo frame as in [Figure 1], demonstrating right-to-left shunt (blue flow) across the ventricular septal defect (VSD) (arrow). Other abbreviations are the same as in [Figure 1]. Reproduced from Ref.[5].

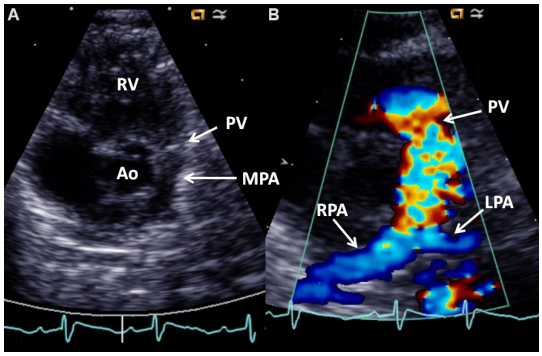

Figure 3. (A) Selected video frame from a 2D echocardiogram in a parasternal short-axis view demonstrating a large aorta (Ao) in the center with thickened pulmonary valve (PV) leaflets and a small main pulmonary artery (MPA) to the left of the Ao. The origins of the branch pulmonary arteries are seen. (B) Color Doppler flow mapping of an echo frame similar to (A) (but magnified) demonstrating color flow disturbance beginning proximally to the PV (arrow). The right (RPA) and left (LPA) pulmonary arteries are more clearly seen in color. Reproduced from Ref.[5]. RV: Right ventricle.

be shown in the echo-Doppler studies. The sizes of the main PA and proximal portions of the branch PAs are appraised by both the two-dimensional (2D) echo and color Doppler [Figure 3]. Nevertheless, it must be noted that the distal PAs are not easy to demonstrate by echographic examination. The RV outflow narrowings might be located in the infundibular region, pulmonary valve, PA above the valve, and branch

PAs or multiple sites may be involved. These obstructive sites should be identified by color, pulsed and continuous wave (CW) Doppler examination. The pulmonary outflow tract obstruction produces elevated Doppler flow velocity through these sites [Figure 4]. But it should be understood that: (1) the neonates usually have high PA pressure and consequently, the pressure gradients by Doppler under-estimate the magnitude of obstruction; and (2) in subjects with very severe pulmonary outflow tract narrowing, the gradients by Doppler may not capture the severity of obstruction because of the limitations imposed by the normal blood pressure and systemic vascular resistance. Careful evaluation of proximal coronary arteries (CAs) must also be undertaken. Anomalous origin of left anterior descending CA from the right CA traversing the RV outflow tract occurs in approximately 5% of patients with TOF[9]. Other coronary anomalies also exist. In cases where proximal CA structure cannot be demonstrated, other imaging investigations, namely, magnetic resonance imaging (MRI), computed tomography (CT) or coronary angiography, may be required prior to surgical correction.

Type II. TOF with pulmonary atresia

Inner heart structure is the same as that depicted above for classic tetralogy. However, the RV outflow region is totally obstructed, i.e., pulmonary atresia, and, as a result, blood flow going from the RV to the PA is not present. The site of atresia may be in the infundibulum, at the valve, or of the main PA, or a mixture of the above. Infrequently, atresia confined only to the pulmonary valve is seen [Figure 5]. The branches of the PAs are usually hypoplastic (or small) and rarely normal in size. These babies are obviously ductal-dependent. In most of such babies, a patent ductus arteriosus (PDA) is present and the PDA is generally long and tortuous.

On echocardiography, the findings of a large VSD, aortic override, and right to left shunt via the ventricular defect [Figures 1 and 2] are the same as those described for classic TOF. The flow of blood through the RV outflow tract is not seen. Valvar atresia may sometimes be demonstrated in echo studies [Figure 5]. The diameters of the main and branch PAs may be demonstrated by 2D echo [Figures 5 and 6] and color flow imaging [Figure 6A]; they are usually small and hypoplastic. In some patients, other imaging techniques such as MRI, CT, or angiography are required to delineate the PA structure. The ductus arteriosus is usually demonstrated by color Doppler studies, and as mentioned, it is usually long and tortuous.

Type III. TOF with multiple aorto-pulmonary collateral arteries

The pathologic structure of the heart is comparable to that portrayed above for tetralogy with pulmonary atresia. There is no onward blood flow from the RV outflow tract into the PAs. The main PA is either very small or absent. The PA branches are diminutive with many stenotic lesions. There is no continuity between the right PA (RPA) and left PA (LPA), and different lobar branches may not be connected to each other. Nevertheless, in some subjects with tetralogy and MAPCAs, hypoplastic central pulmonary arteries connect to the RPA and LPA. However, in the majority of patients, the flow of blood to the lungs is mostly provided by MAPCAs. The distribution of these vessels is variable and complex[10]. They are abnormal and connect the systemic arteries with PAs. The MAPCAs usually originate from the branches of the aorta. The origin of these vessels may be either from above or below the diaphragm level. They frequently have circuitous courses, cross the midline and supply the central, lobar, and segmental PAs, and may connect distal to stenotic lesions or discontinuous vessels. The MAPCAs are usually tortuous and uneven in diameter, and frequently have stenotic lesions within themselves. Despite having multiple vessels supplying the lungs, pulmonary perfusion is disorderly and inefficient. The majority of babies have decreased blood flow to the lungs with variable grades of hypoxemia. A few children, however, may have increased pulmonary blood flow, though this is less common. Infrequently, a small PDA may be present, but in the classic type of MAPCAs, PDA is not seen.

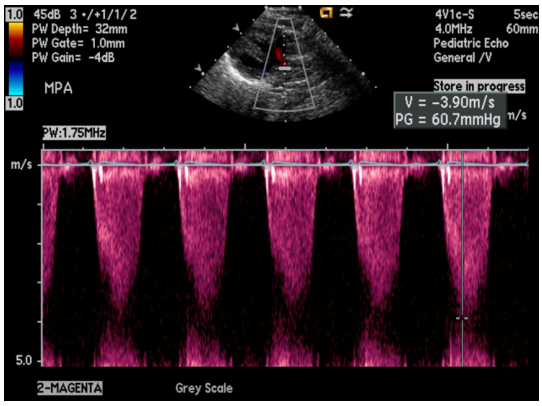

Figure 4. Increased Doppler flow velocity (3.9 m/s) across the right ventricular outflow tract demonstrating severe obstruction; the calculated gradient by modified Bernoulli equation is 60.7 mmHg (insert). Reproduced from Ref.[5]. PG: Peak gradient; PW: pulse width; V: Doppler flow velocity.

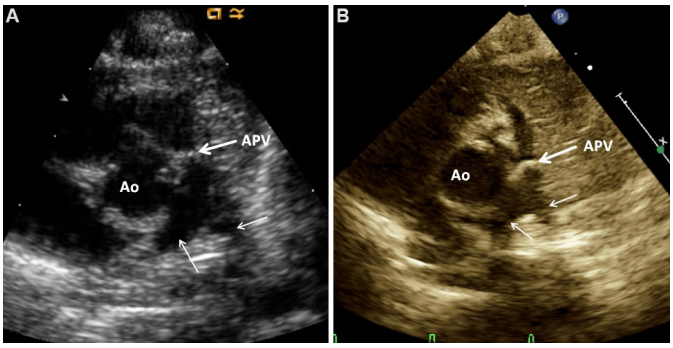

Figure 5. Selected video frames from a 2D echocardiogram in parasternal short-axis views in two different neonates (A) and (B) demonstrating a large aorta (Ao) in the center and atretic pulmonary valve (APV; thick arrows) and small main, left (LPA), and right (RPA) pulmonary arteries (thin arrows). Reproduced from Ref.[5].

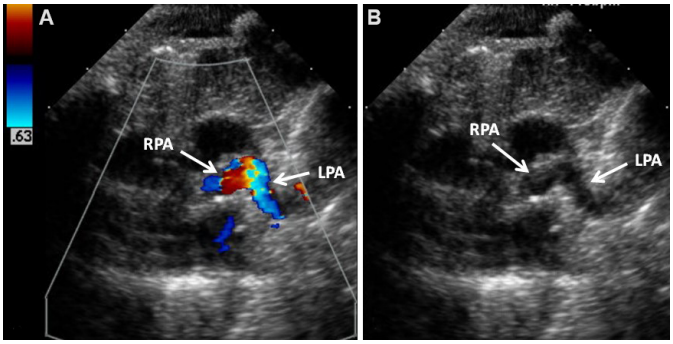

Figure 6. Selected video frames from a 2D echocardiogram (B) and color flow mapping (A) in a parasternal short-axis view demonstrating small left (LPA) and right (RPA) pulmonary arteries (arrows). Reproduced from Ref.[5].

In echocardiographic studies, the internal cardiac structure is similar to that observed with Types I and II TOF cases [Figures 1 and 2]. Pulmonary atresia is suggested by Doppler interrogation, indicating an absence of blood flow originating from the RV and ending into the PA. The branch PAs are frequently very hypoplastic and may not be evident on echocardiography. Aorto-pulmonary collateral vessels may at times be identified by a continuous flow pattern in pulsed Doppler and on color flow imaging [Figure 7]. Careful

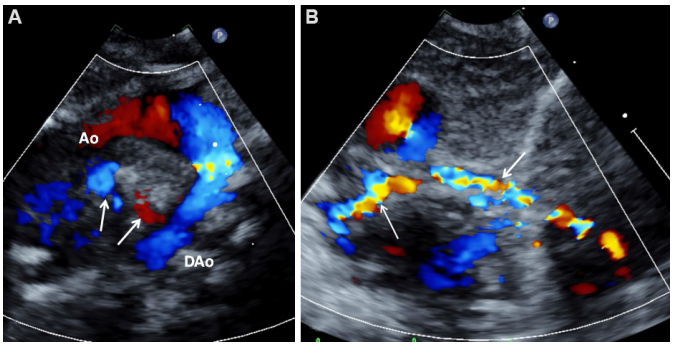

Figure 7. Selected video frames from color flow mapping images in suprasternal notch views demonstrating collateral vessels marked with arrows both in (A) and (B). Reproduced from Ref.[5]. Ao: Aorta; DAo: descending aorta.

interrogation may illustrate where the large collateral vessels may arise, but where they empty into the PAs is difficult to demonstrate. In addition, small-sized collateral vessels may be difficult to see. Most usually, echocardiography by itself is not adequate to reveal important aspects of the anatomy of the PAs and how the blood supply to all segments of the lungs is distributed in these cases of TOF with MAPCAs. Computed tomography and/or selective cine-angiography are often necessary to demonstrate these abnormalities[5,6].

Type IV. TOF with syndrome of absent pulmonary valve

Syndrome of absent pulmonary valve is an uncommon heart defect and makes up 3% to 5% of all cases of TOF. It comprises of: (1) rudimentary leaflets of the pulmonary valve, with consequent pulmonary insufficiency; (2) pulmonary valve annular hypoplasia, producing PS; and (3) marked dilatation (aneurismal) of the main and major branch PAs, producing variable amounts of tracheo-bronchial tree compromise. Inner cardiac structure is reasonably akin to that found with Types I, II, and III TOFs described in the preceding sections of this paper. However, infundibular obstruction is rare. Also, the ductus arteriosus is absent in the majority of cases. This syndrome is typically seen in association with TOF, even though it may infrequently be found as a sole abnormality. Other defects may also be encountered with this syndrome: ASD, VSD, atrioventricular septal defect, and double outlet right ventricle (DORV)[5,6,11].

An echocardiogram shows a large VSD and over-riding aorta; such findings are similar to those seen with the preceding three types of TOF [Figures 1 and 2]. Rudimentary or absent leaflets of the pulmonary valve and hypoplasia of the pulmonary valve ring may also be detected [Figure 8]. Color flow imaging demonstrates turbulent flow through the pulmonary valve [Figure 9A] with pulmonary insufficiency [Figure 9B]. CW Doppler studies demonstrate an increased Doppler flow velocity indicative of a high pulmonary valve peak systolic pressure gradient and evidence for pulmonary insufficiency [Figure 10]. The main and branch PAs are aneurismally dilated; this can be documented on 2D echocardiograms [Figure 8].

TRANSPOSITION OF THE GREAT ARTERIES

Transposition of the great arteries (TGA) comprises 5% of all heart defects and accounts for 10% of all cyanotic neonates. Indeed, TGA is the utmost frequent cyanotic heart defect in neonates[3,4,12,13]. In TGA, the PA arises from the morphologic left ventricle (LV) while the aorta comes off of the morphologic RV. In the utmost common variety - called complete TGA - normal position of the atria (atrial situs solitus) is present, the right atrium (RA) is connected to the RV and the left atrium (LA) is connected to the LV [atrioventricular (AV) concordance], the RV is on the right and the LV on the left (d-loop of the ventricles), and the aorta arises from the RV and the PA from the LV (ventriculo-arterial discordance). Most

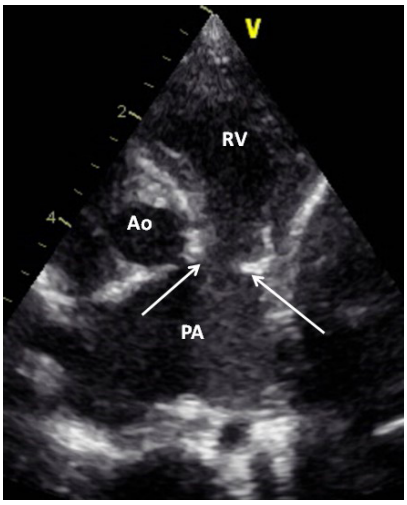

Figure 8. Selected video frame from a 2D echocardiogram in a parasternal short-axis view demonstrating rudimentary pulmonary valve leaflets (arrows) and dilated main and proximal portions of the right and left pulmonary arteries. Reproduced from Ref.[5]. Ao: Aorta; PA: pulmonary artery; RV: right ventricle.

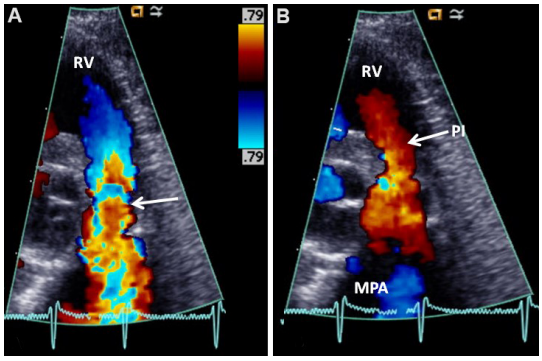

Figure 9. Selected video frames from color flow mapping in a parasternal short-axis view demonstrating turbulence originating at the pulmonary valve ring level (arrow in A) and pulmonary insufficiency (PI; arrow in B). Reproduced from Ref.[5]. MPA: Main pulmonary artery; RV: right ventricle.

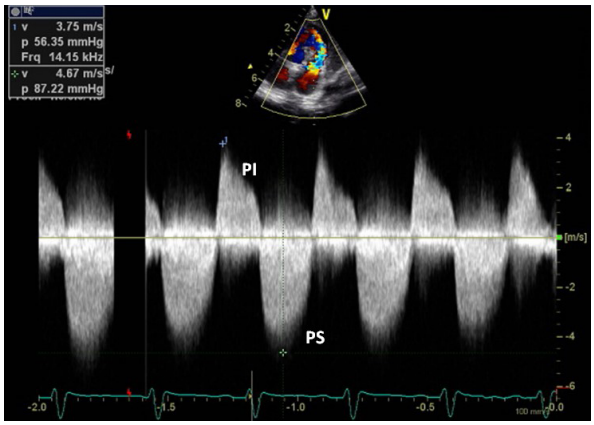

Figure 10. Continuous wave Doppler recording across the right ventricular outflow tract in the same patient as shown in [Figures 8 and 9] demonstrates a severe gradient across the pulmonary outflow tract (87 mmHg - see insert) and pulmonary insufficiency (PI). Reproduced from Ref.[5]. PS: Pulmonary stenosis.

commonly, the aortic valve is situated to the right of the pulmonary valve, which is termed d-TGA. As a result, the systemic venous blood from the superior and inferior vena cavae empties into the RA and is then transported to the RV and from there into the aorta, while the pulmonary venous blood empties into the LA and from there transported to the LV and then ejected into the PA. Hence, the TGA patient's circulatory pattern is parallel in place of the normal circulation which is in-series. This state of circulatory abnormality results in not conveying the pulmonary venous blood return to the body and not delivering the systemic venous return to the lungs. Given this type of circulatory anomaly, the neonates have no chance to survive unless there is mixing between both circulations through persistent fetal pathways, for instance, patent foramen ovale (PFO) and PDA, or an ASD or VSD[3,4,12-14].

Because of differences in presentations and the types of management required, we have arbitrarily classified TGA into[12,13]: (1) Group I, TGA with intact ventricular septum; (2) Group II, TGA with VSD; and (3) Group III, TGA with VSD and PS.

Group I, TGA with intact ventricular septum

Echocardiograms are valuable in the diagnosis of TGA and in the evaluation of co-existing cardiac defects. Since the anatomy of the atria and ventricles is normal, as well as those of the semilunar (aortic and pulmonary) valves, the identification of transposition may be a bit tricky by echocardiogram, mostly for the novice. An incidental sign is a slightly posterior passage of the artery arising from the LV in a parasternal long-axis projection [Figure 11A], signifying that this artery is likely to be the PA, is useful. Such an appearance is in contrast to an anteriorly traversing proximal aorta [Figure 11B] in normal neonates. When the blood vessel coming off of the LV is followed, and its division into branch PAs is shown [Figure 12], that artery is recognized as PA with consequent confirmation of the finding of transposition. Additional signs that are useful and indicative of transposition are a parallel positioning of the aorta and PA in an echocardiographic long-axis projection [Figures 11A and 13A] and a concurrent on-end imagining of both the aortic and pulmonary valves on a parasternal short-axis projection [Figure 13B].

The inter-atrial septum must be assessed in the subcostal projections by 2D [Figure 14A] and color flow Doppler [Figure 14B and C]. The atrial defect is typically a PFO and rarely, a true ASD may be seen. An atrial defect that is 5 mm or more in diameter is commonly deemed sufficient for the provision of adequate admixture of blood across the atrial septum and for the avoidance of balloon atrial septostomy.

PDA may also be seen and the shunting via the ductus by pulsed, CW, and color [Figures 15 and 16] Doppler should be ascertained.

Group II. TGA with VSD

Group II TGA babies characteristically manifest signs and symptoms indicative of congestive heart failure and their presentation is much later than the babies with intact ventricular septum. Echocardiographic studies are useful in diagnosing TGA [Figures 11-13] and in identifying size and shunt across the VSD [Figure 17].

Group II. TGA with VSD and PS

The timing of presentation of babies with transposition associated with VSD and PS (Group III) varies, largely based on the degree of inter-circulatory blood admixture and the degree of PS. Echocardiographic studies are helpful in the visualization of VSD and PS [Figure 18]. Shunts across the ventricular defect by color Doppler imaging [Figures 18A and B] and extent of narrowing of the pulmonary outflow tract by pulsed, CW, and color [Figure 18] Doppler must be assessed and such an evaluation is useful in evaluating the physiologic status of the infant.

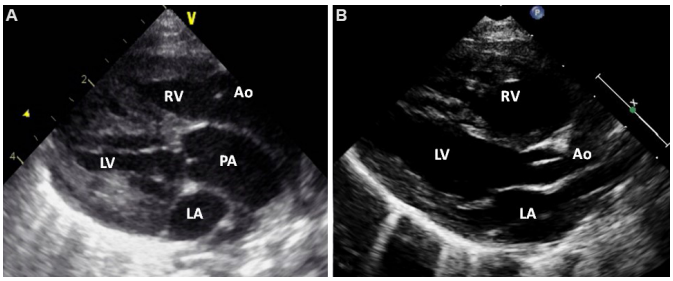

Figure 11. Parasternal long-axis echocardiographic views of two neonates, first, (A), with transposition of the great arteries and second, (B), with normally related great arteries. Note that in (A), the posterior vessel arising from the left ventricle (LV) is coursing backward (posteriorly) after its origin from the LV and is likely to be the pulmonary artery (PA), suggesting transposition of the great arteries. This vessel should be traced and its bifurcation demonstrated (see Figure 12) to confirm that it is indeed the PA. In (B), the posterior vessel arising from the LV courses somewhat anteriorly, indicating that it is likely to be the aorta. Reproduced from Ref.[13]. Ao: Aorta; LA: left atrium; RV: right ventricle.

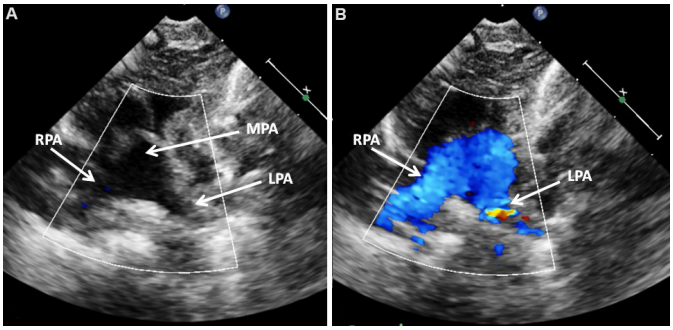

Figure 12. The vessel arising from the left ventricle of the infant shown in [Figure 11A] was traced, which showed bifurcation in 2D (A) and color flow (B) images into the right (RPA) and left (LPA) pulmonary arteries suggesting that this vessel is the main pulmonary artery (MPA), confirming the diagnosis of transposition of the great arteries. Reproduced from Ref.[13].

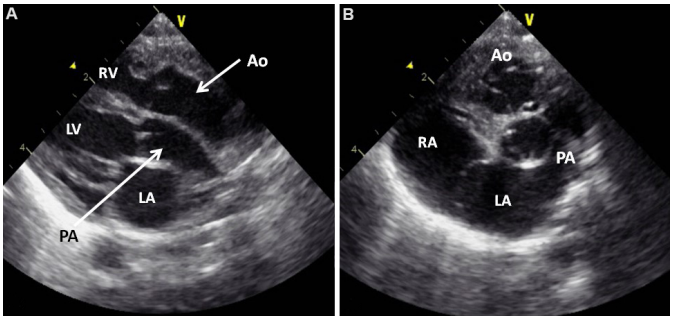

Figure 13. Selected video frames from a 2D echocardiogram in long (A) and short (B) axis views of an infant with transposition of the great arteries. Note the parallel position of the pulmonary artery (PA) and aorta (Ao) in A and on-end visualization of PA and Ao in (B). These echoes are highly suggestive of transposition of the great arteries; in a normal baby, because of the normal crisscrossing of the PA and Ao, such an appearance is unlikely. Reproduced from Ref.[13]. LA: Left atrium; LV: left ventricle; RA: right atrium; RV: right ventricle.

Balloon atrial septostomy

The effect of Rashkind balloon atrial septostomy is easily evaluated by echo-Doppler studies both in the catheterization laboratory immediately following balloon septostomy and during follow-up. Improvement in 2D diameter of the atrial defect [Figure 19] and favorable color Doppler shunt characteristics [Figure 20] following septostomy can be demonstrated[13,14].

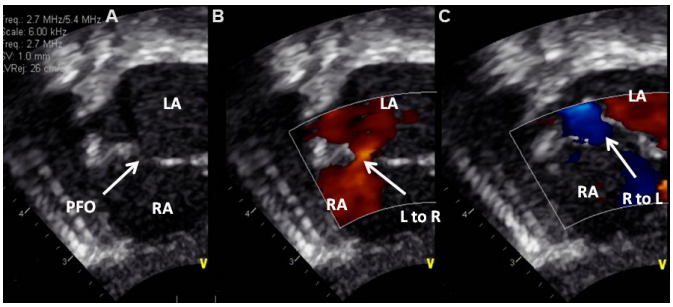

Figure 14. Selected video frames from subcostal views of a neonate with transposition of the great arteries demonstrating patent foramen ovale (PFO). (A) Demonstrates PFO by 2-dimensional imaging. (B, C) show: a left to right (L to R) shunt in (B) and right to left (R to L) shunt in (C) in different phases of the cardiac cycle. Reproduced from Ref.[13]. LA: Left atrium; RA: right atrium.

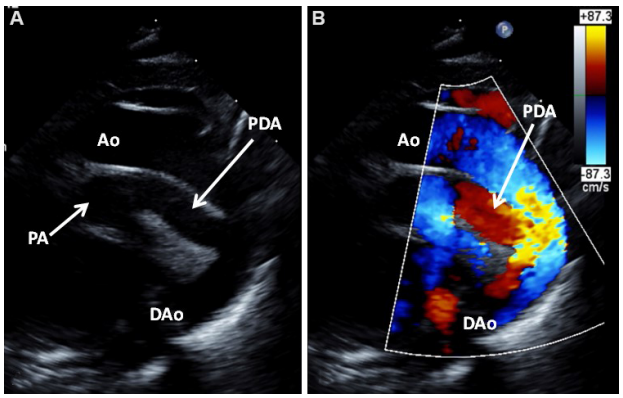

Figure 15. Selected video frames from suprasternal notch views of the aortic (Ao) arch of a neonate with transposition of the great arteries demonstrating a large patent ductus arteriosus (PDA); 2D (A) and color flow images (B) are shown. Reproduced from Ref.[13]. DAo: Descending aorta; PA: pulmonary artery.

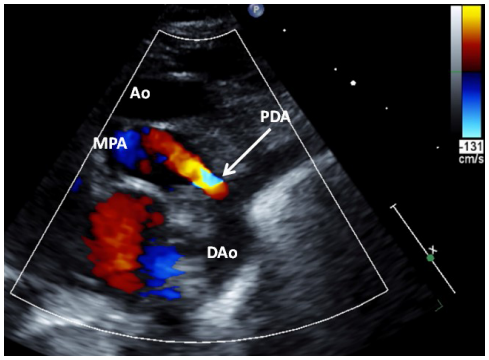

Figure 16. Selected video frame from suprasternal notch views of the aortic (Ao) arch of another neonate with transposition of the great arteries demonstrating a small patent ductus arteriosus (PDA). Reproduced from Ref.[8]. DAo: Descending aorta; MPA: main pulmonary artery.

TRICUSPID ATRESIA

Tricuspid atresia (TA) is a cyanotic heart defect and is described as a congenitally absent or lack of development (agenesis) of the morphological tricuspid valve[15-18]. TA is the 3rd most frequent cyanotic heart defect and constitutes 1.4% to 1.5% of all CHDs[17]. There is atresia of the tricuspid valve. In the utmost frequent muscular type, the atretic tricuspid valve is visualized as an indentation or a local fibrous knob in

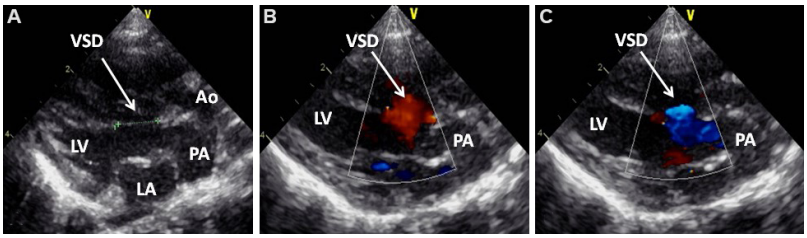

Figure 17. Selected video frames from parasternal long-axis views of a neonate with transposition of the great arteries demonstrating a large (A) ventricular septal defect (VSD) with bidirectional shunting (B, C). Reproduced from Ref.[13]. Ao: Aorta; LA: left atrium; LV: left ventricle; PA: pulmonary artery.

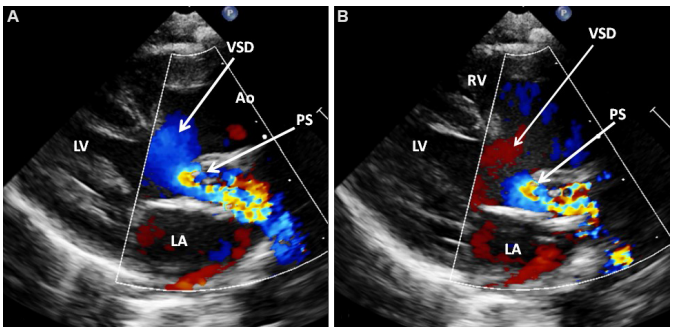

Figure 18. Selected video frames from parasternal long-axis views of a neonate with transposition of the great arteries demonstrating a large ventricular septal defect (VSD) and severe pulmonary stenosis (PS). Right to left (A) and left to right (B) shunts across the VSD are shown. Reproduced from Ref.[13]. Ao: Aorta; LA: left atrium; LV: left ventricle; RV: right ventricle.

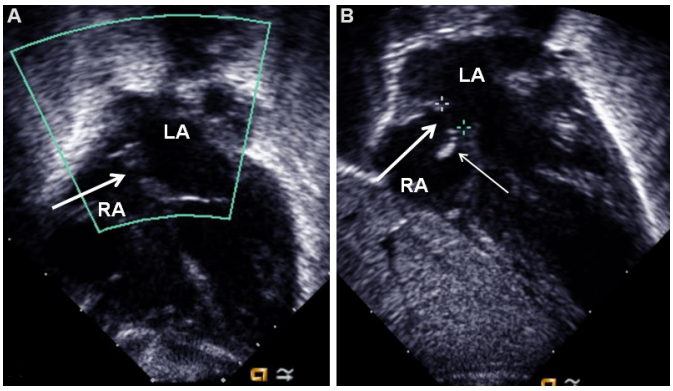

Figure 19. Selected video frames from subcostal views, demonstrating a small inter-atrial opening (arrow in A) which became larger (thick arrow in B) after Rashkind balloon atrial septostomy. The thin arrow in (B) points to the torn flap of the lower margin of the patent foramen ovale. The left and right ventricles are not labeled. Modified from Ref.[14]. LA: Left atrium; RA: right atrium.

the flooring of the RA at the expected location of the orifice of the tricuspid valve. Other anatomic types, such as membranous, valvar, Ebstein's, AV septal, and unguarded with muscular shelf, have also been described[15]. The RA is dilated. An atrial defect, typically a stretched PFO, is seen. Occasional patients may have ASDs of ostium secundum or an ostium primum variety. The LA is dilated, particularly in patients with increased blood flow to the lungs. The mitral valve generally has two valve leaflets (bicuspid) with morphological characteristics of a mitral valve. Nevertheless, its opening is big and infrequently regurgitant. The LV is clearly morphologic LV; however, it is dilated and hypertrophied. Hypoplasia of the RV is usually seen and the RV size is inadequate to sustain pulmonary circulation. The great vessel relationship is variable

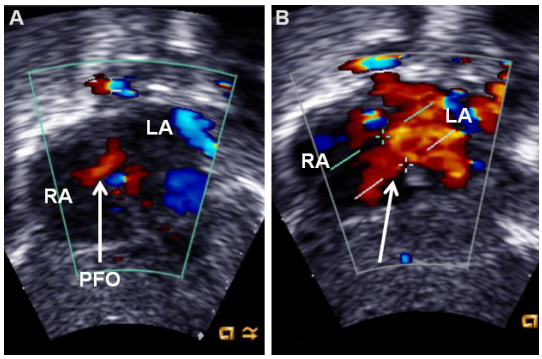

Figure 20. Selected video frames from subcostal long-axis views of the atrial septum, demonstrating a small color flow jet across the patent foramen ovale (PFO; arrow in A), which was enlarged (arrow in B) after balloon atrial septostomy. The jet width is wider, and the flow is laminar after balloon septostomy. Modified from Ref.[14]. LA: Left atrium; RA: right atrium.

and forms the source for classifying this lesion[15]: (1) Type I, normally related great vessels; (2) Type II, d-TGA; (3) Type III, malpositions of the great vessels other than d-transposition; and (4) Type IV, common truncus[15]. The proximal aorta may be normal in diameter or somewhat bigger than usual. The RV outflow tract is normal, stenosed, or atretic; this forms the basis of the subgrouping of TA[15]. A VSD is usually seen, although an occasional patient may have an intact ventricular septum. When a ventricular defect is present, it may be big, medium or small, or many VSDs may be seen. The VSD is typically located in the muscular component of the ventricular septum. Most of the ventricular defects are restrictive and produce obstruction in the sub pulmonary region in Type I cases with normal great artery relationship and subaortic stenosis in the Type II cases with transposed great arteries. In patients who have pulmonary atresia, the blood flow to the lungs is provided via a PDA; in the absence of PDA, one or more aorto-pulmonary collateral vessels may supply the lungs.

An echocardiographic examination is valuable in making the diagnosis and in defining multiple structural and hemodynamic issues[18-21]. In the most frequent muscular variety, the blocked tissue of the tricuspid apparatus is imaged as a compact band of echo images at the usual location of the tricuspid valve [Figure 21]. Subcostal and apical four-chamber projections are best to demonstrate the anatomic details. Other anatomic types can also be demonstrated on echocardiography, although rare. Dilated atria (both right and left) and LV and a hypoplastic RV are visualized on 2D echocardiography.

Echo-Doppler study is also helpful in demonstrating the shunt from the right atrium to the left via the PFO/ASD [Figure 22] and left to right shunt via the VSD [Figure 23]. The VSD may be shown by 2D imaging [Figure 23A]. The shunt via the defect is demonstrated by color flow imaging [Figure 23B] and pulsed and CW [Figure 23C] Doppler interrogation. Increased Doppler flow velocity through the RV outflow tract (RVOT) and the pulmonary valve will help demonstrate obstruction at these locations. The Doppler information from the VSD [Figure 23C] and RVOT is valuable in estimating the pressures in the PA.

As mentioned above, TA is classified on the basis of the great artery relationship. The most common forms are: (1) Type I, normally related great vessels; and (2) Type II, d-transposition of the great vessels. The relationship of the great vessels is established by tracing the vessels until bifurcation [Figure 24] or aortic arch, as reviewed in the TGA section above.

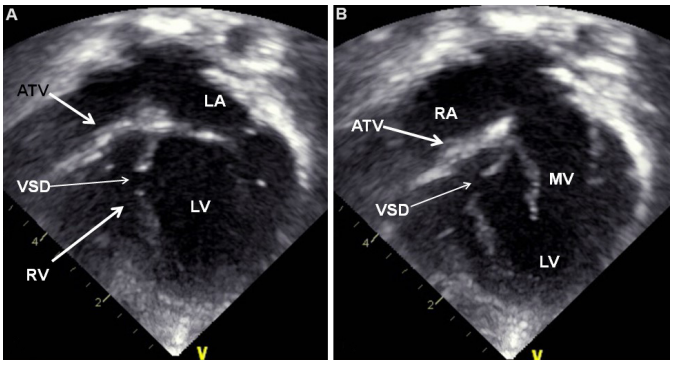

Figure 21. Selected video frames from apical four-chamber, 2-dimensional echocardiographic views of a patient with tricuspid atresia showing an enlarged left ventricle (LV), a small right ventricle (RV), and a dense band of echoes at the site where the tricuspid valve echo should be (ATV; thick arrow) with closed (A) and open (B) mitral valve during LV systole and diastole, respectively. A moderate-sized ventricular septal defect (VSD; thin arrow) is shown. Reproduced from Ref.[19]. ATV: Atretic tricuspid valve; LA: left atrium; RA: right atrium.

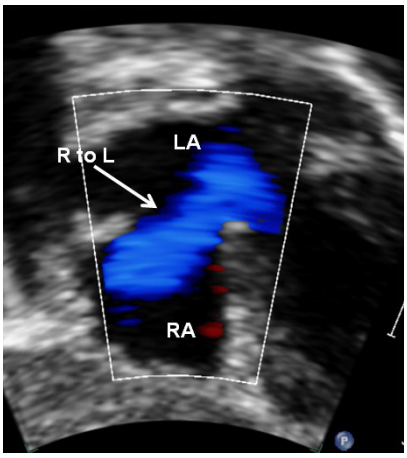

Figure 22. Selected video frame from the subcostal view of a patient with tricuspid atresia demonstrating the right to left (R to L) shunt (thick arrow) across the interatrial communication. Reproduced from Ref.[19]. LA: Left atrium; RA: right atrium.

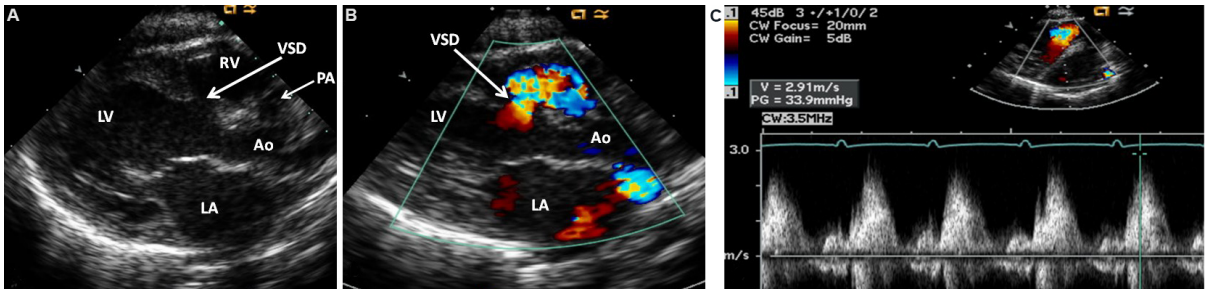

Figure 23. Selected video frames from parasternal long-axis views of a patient with tricuspid atresia with normally related great arteries demonstrating enlarged left atrium (LA) and left ventricle (LV), a small right ventricle (RV), and a moderate-sized ventricular septal defect (VSD; thick arrow) on 2D (A) and color flow (B) imaging. Turbulent flow (B) with a Doppler flow velocity of 2.91 m/s by continuous wave Doppler (C) suggests some restriction of the VSD. Reproduced from Ref.[19]. Ao: Aorta; PA: pulmonary artery.

In subjects with Type I (normally related great vessels), the ventricular defect provides blood flow into the lungs [Figure 23]. In these cases, the highest Doppler flow velocity through the VSD is useful in estimating

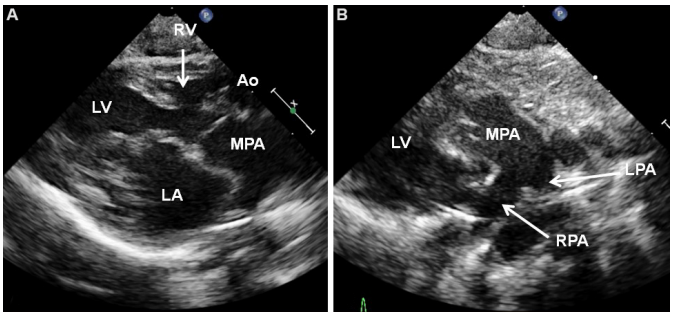

Figure 24. (A) Selected video frame from parasternal long-axis views of a baby with tricuspid atresia and transposition of the great arteries demonstrating left atrium (LA), left ventricle (LV), a very small right ventricle (RV), and a moderate-sized ventricular septal defect (not marked). The vessel coming off of the LV shown in A is traced in (B) and demonstrated to bifurcate into left (LPA) and right (RPA) pulmonary arteries, confirming that this vessel is the main pulmonary artery (MPA). Reproduced from Ref.[19]. Ao: Aorta.

the VSD size; the greater the velocity, the smaller the defect. The RV and PA pressures in systole may also be appraised utilizing a simplified Bernoulli formula:

Systolic pressure in the RV and PA = systolic BP - $4V^2$

where V is the VSD peak Doppler velocity, RV is the right ventricle, PA is the pulmonary artery, and BP is the blood pressure in the arm.

In subjects with elevated pulmonary artery pressures and marked stenosis at the infundibular or valvar level, the Doppler flow velocities across the VSD do not reflect the VSD size.

In Type II (TGA) patients, the VSD provides systemic flow. If the ventricular defect is small, it produces obstruction to systemic flow. Therefore, the VSD size should be assessed by 2D [Figure 24], color [Figure 25], pulsed [Figure 26], and CW Doppler as deemed appropriate. In Type II (transposition) subjects, an elevated VSD Doppler velocity suggests obstruction in the subaortic region.

Doppler interrogation of the RVOT in Type I subjects and the PA area in Type II children is likely to disclose sub pulmonary or pulmonary valve obstruction; the greater the velocity, the more severe the stenosis.

Echo-Doppler examination from suprasternal notch view may demonstrate aortic coarctation [Figure 27]; coarctation is more frequent in subjects with associated TGA (Type II).

2D imaging along with bubble contrast with agitated saline or similar contrast materials may clearly show successive visualization of the right and left atria, LV, and then the RV in that sequence; however, such an examination is not needed in the diagnosis of TA.

The findings on echo-Doppler studies are amply characteristic for TA and consequently, catheter studies with angiograms are not needed to confirm the diagnosis.

TOTAL ANOMALOUS PULMONARY VENOUS CONNECTION

In total anomalous pulmonary venous connection (TAPVC), most of the time, all pulmonary veins are connected to a common pulmonary vein (CPV) which in turn drains into various systemic venous

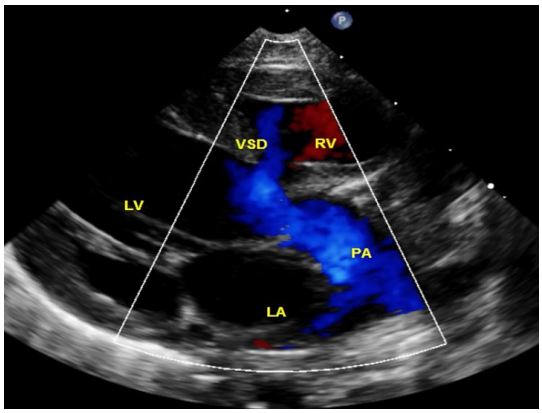

Figure 25. Selected video frame from parasternal long-axis view with color flow mapping of another patient with tricuspid atresia and transposition of the great arteries demonstrates left atrium (LA), left ventricle (LV), a small right ventricle (RV), and a moderate-sized ventricular septal defect (VSD). The vessel coming off the LV bifurcates. Reproduced from Ref.[19].

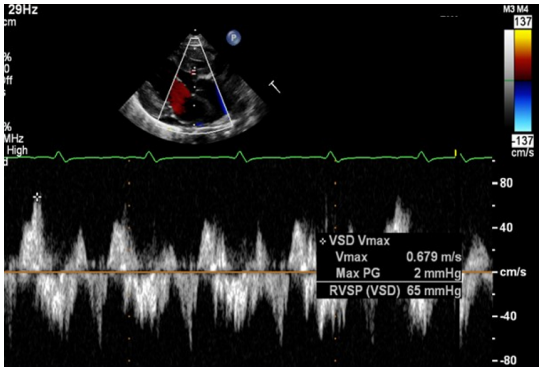

Figure 26. Selected video frame of continuous wave Doppler across the ventricular septal defect of the same patient as shown in [Figure 25]. Low velocity flow across the ventricular septal defect (VSD) suggests that the defect is non-obstructive. Reproduced from Ref.[19]. Vmax: Maximum velocity; PG: peak gradient; RSVP: right ventricular systolic pressure.

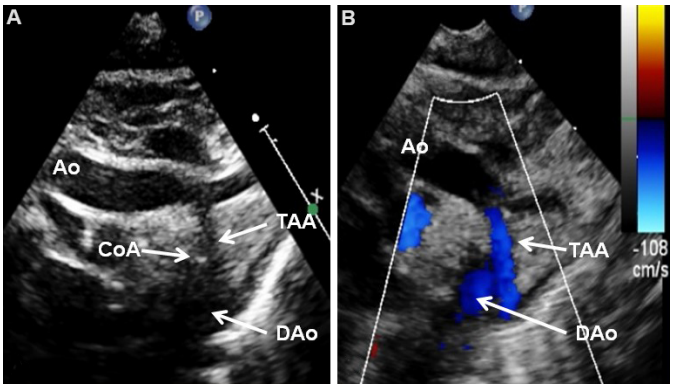

Figure 27. Selected video frames from suprasternal notch views of the aortic (Ao) arch in 2D (A) and color flow (B) images of a neonate with tricuspid atresia and transposition of the great arteries demonstrating coarctation of the aorta (CoA) and hypoplastic transverse aortic arch (TAA). The association of CoA with tricuspid atresia plus transposition of the great arteries is well known. Reproduced from Ref.[19]. DAo: Descending aorta.

structures. Less commonly, each pulmonary vein may directly connect to the RA, or the pulmonary veins

drain into multiple sites. Most frequently, the common pulmonary vein drains into the left innominate vein. Other connection sites are: superior vena cava, coronary sinus, portal vein, or other unusual places[4,22-24]. The TAPVC is the fifth most frequent cyanotic CHD accounting for 2% to 3% of all CHDs. Two classifications of TAPVC exist, the first is based on the site to which the connecting anomalous vein drains[25,26] and the second is based on physiology, i.e., obstructive and non-obstructive[26,27]. As per the first classification, they are supra-cardiac in 45%, cardiac in 25%, infra-cardiac in 25%, and mixed in 5% cases. Connection of the CPV to the left innominate vein is the utmost common type among all cases of TAPVC while the drainage into a structure below the level of diaphragm (infra-diaphragmatic) is the most common variety in a symptomatic newborn. The classification based on physiology (obstructive and non-obstructive) is helpful in clinical recognition and management. Supra-diaphragmatic TAPVC is usually non-obstructive, although obstruction lesions have been reported in this group also, as discussed elsewhere[27]. On the other hand, obstruction is universal in infra-diaphragmatic TAPVC patients.

The entirety of the pulmonary venous return ultimately drains into the RA in all types of TAPVC. Hence, the admixture of the pulmonary and systemic venous returns (plus the blood return from the coronary sinus) occurs in the RA. Consequently, shunting from the RA to LA through the PFO (or ASD) is necessary to provide systemic flow. The relative flow distribution to systemic (via the PFO) and pulmonary (via the tricuspid valve) circulations is reliant on the respective compliances of the RV and LV.

Echo-Doppler examination is helpful in establishing the diagnosis of TAPVC and assessing central issues relevant in the treatment of these infants[22,24]. In normal babies, the connection of the pulmonary veins to the LA is easily shown in the suprasternal notch crab-view [Figure 28]. Other views also can demonstrate the entrance of the pulmonary venous structures into the LA. If the entrance of pulmonary veins into the LA by color Doppler cannot be demonstrated, the possibility of TAPVC should be considered. Also, when there is marked elevation of the RV/PA pressures [Figure 29A] and/or a pure right to left shunt through the PFO [Figure 29B], a diagnosis of TAPVC should be suspected. However, it should be noted that these findings can also be present in babies with persistent pulmonary hypertension and at times in babies with severe aortic coarctation.

The right heart structures (RA, RV, and PA) are dilated in all varieties of TAPVC [Figure 30] while the LA and LV generally look smaller than the right heart structures. A smaller LA than normal may in part be related to no contribution of the CPV to the LA size; however, it is easily visualized [Figure 30A, B and D]. The LV appears to be compressed posteriorly [Figure 30A and C] and to the left [Figure 30D] by the enlarged RV.

The RV and PA systolic pressures are increased, particularly in the infra-diaphragmatic types, and can be shown by a markedly increased tricuspid insufficiency jet velocity [Figure 29A]. A simplified Bernoulli formula may appraise these pressures:

RV and PA systolic pressure = $4V^2 + 5$ mmHg

RV, right ventricle; PA, pulmonary artery; V, the peak velocity of tricuspid insufficiency jet; and 5 mmHg is assumed pressure in the PA.

Shunting from the RA to LA through the PFO is also present in all varieties of total veins [Figure 29B].

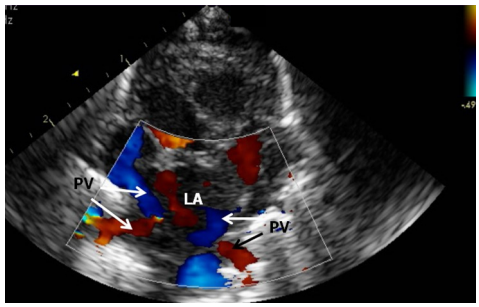

Figure 28. Suprasternal notch crab-view of the pulmonary veins (PV) draining into the left atrium (LA) are shown by color flow imaging. The LA is in the center with four PVs showing color flow; the upper PVs show blue color while both lower PVs show red color. Each of the PVs is also pulse-Doppler interrogated during any routine study and normal Doppler velocity recorded (not shown). Reproduced from Ref.[21].

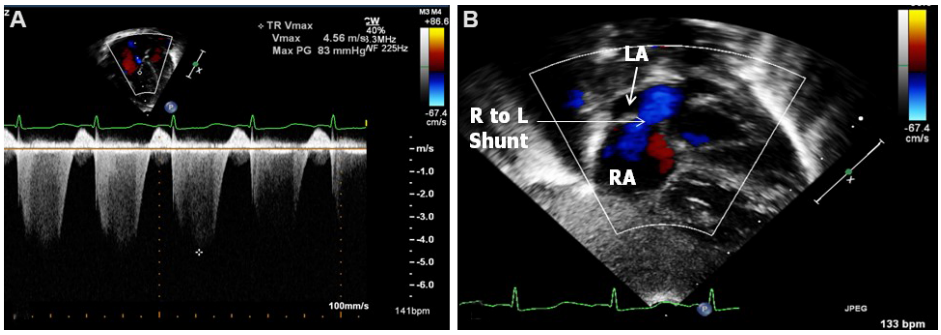

Figure 29. (A) A high tricuspid regurgitant Doppler flow velocity is shown and is suggestive of elevated pulmonary artery pressure in a neonate with the infra-diaphragmatic type of total anomalous pulmonary venous connection. (B) Color Doppler flow mapping demonstrating right-to-left shunting across the atrial septum. Reproduced from Ref.[21]. RA: Right atrium; LA: left atrium.

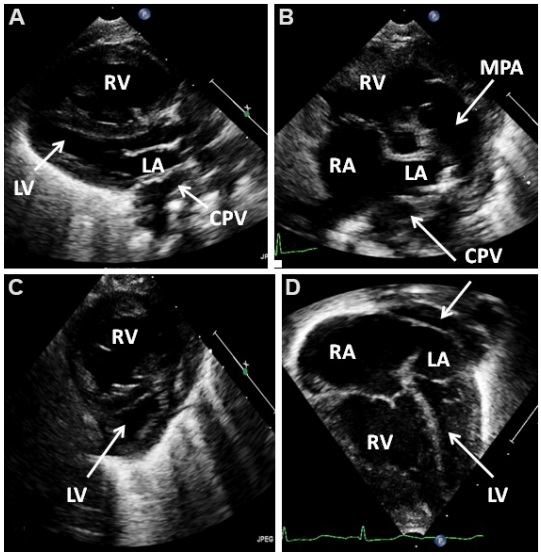

Figure 30. Selected video frames of a 2-dimensional echocardiogram in parasternal long- (A) and short- (B, C) axis and apical four chamber (D) views demonstrating a large right atrium (RA), right ventricle (RV), and main pulmonary artery (MPA) in an infant with total anomalous pulmonary venous connection. Note that the enlarged RV encroaches onto the left ventricle compressing it posteriorly (A, C) and to the left (D). The common pulmonary vein (CPV) is located behind (A, B) and superior to the left atrium (LA) (D). Reproduced from Ref.[24].

The CPV may be visualized posterior to the LA [Figure 30A and B]. It may also be imaged superior to the LA in apical four-chamber view [Figure 30D]. Every attempt must be exerted to show the entrance of all pulmonary veins into the CPV by means of combined 2D echo and color Doppler [Figure 31] in several projections. Subcostal, parasternal, and supra-sternal notch views should be scrutinized to accomplish this. The horizontal or vertical orientation and the size of the CPV should also be demonstrated. The anomalous draining vein should be shown and the site of its connection established by careful color flow imaging.

Several images of TAPVC with drainage into the infra-diaphragmatic site [Figure 32], left innominate vein [Figure 33], and coronary sinus [Figure 34] locations stand illustrated below.

Obstruction of the anomalous connecting vein may be present and should be shown by demonstrating the site of obstruction (segmental obstruction), by an enlarged proximal part of the anomalous connecting vein, and/or by Doppler flow that is turbulent or continuous. Also, the Doppler flow velocity may be high [Figure 35]. Non-obstructed forms have low velocities [Figure 36].

If a PDA is present, right to left shunt via the ductus is typically visualized, especially in babies with obstructed total veins.

Echo-Doppler studies are sufficiently accurate to confirm the diagnosis and guide treatment decisions without resorting to cardiac catheterization and angiography.

TRUNCUS ARTERIOSUS

Truncus arteriosus is a CHD in which only one blood vessel (truncus) originates from the heart and this vessel gives origin to the aorta, PAs and coronary arteries. The truncus overrides a large outlet VSD[4,22,28-30]. In truncus, the formation of atria and ventricles is normal. Collett and Edwards[31] in 1949 described a classification of the truncus on the basis of how PAs are connected to the truncus: (1) Type I. A short main PA comes off of the side of the truncus, which splits into RPA and LPA. Type I is the utmost frequent form of truncus arteriosus and constitutes 50% to 70% of all truncus cases. (2) Type II. The RPA and LPA originate as distinct vessels behind (posterior) the truncus. Type II is the second most frequent type accounting for 30% to 50% cases. (3) Type III. The origin of RPA and LPA is from the side (lateral aspect) of the truncus. Type III is the least frequent type comprising 6 to 10% of all truncus arteriosus cases. (4) Type IV. The pulmonary flow is supplied either via a PDA or MAPCAs originating from the aorta. This entity is also portrayed as pseudotruncus. However, at the present time, Type IV truncus is not considered to be a variety of truncus arteriosus; instead, it is a form of VSD with pulmonary atresia[28-30].

Thickening of the truncal valve leaflets may be seen in some patients. The truncal valve is usually tricuspid with occasional cases exhibiting bicuspid or quadricuspid valve leaflets. Narrowing of the truncal valve in 5% to 10% of cases and regurgitation of the truncal valve in 5% to 20% of cases may be seen. The PAs are not typically narrowed. The absence of one of the PAs may occur in 16% of cases; such an abnormality is generally on the same side where the aortic arch descends, or the PA may come off of the descending portion of the aorta. In unusual patients, one PA comes off of the ascending aorta while the other arises from the RV; this anomaly has been described a hemi-truncus. In nearly 40% of patients, the aortic arch descends on the right side. The frequent association of interruption of the aortic arch and DiGeorge syndrome with truncus is well recognized.

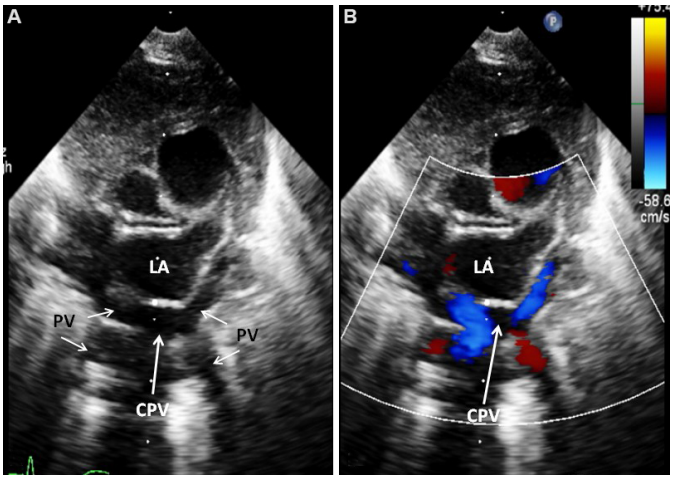

Figure 31. Selected video frames from suprasternal notch views in a baby with the infra-diaphragmatic type of total anomalous pulmonary venous connection showing pulmonary veins (PV) draining into a common pulmonary vein (CPV) which is located posterior to the left atrium (LA); 2-dimensional (A) and color flow mapping (B) images are shown. Modified from Ref.[24].

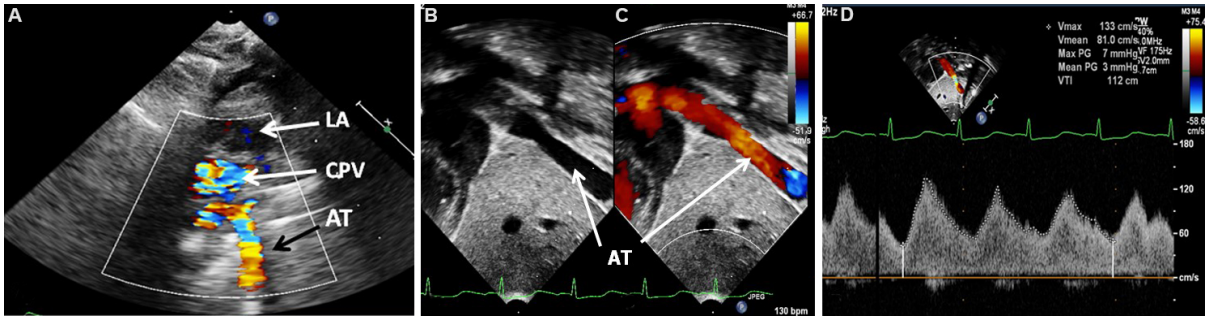

Figure 32. Selected video frames from suprasternal notch (A) and subcostal (B-D) views of an anomalous pulmonary venous trunk (AT) draining the common pulmonary vein (CPV) in a baby with the infra-diaphragmatic type of total anomalous pulmonary venous connection. A continuous wave Doppler recording of the obstructed anomalous trunk demonstrates increased velocity (D) suggesting mild obstruction. Reproduced from Ref.[24]. LA: Left atrium.

Echo-Doppler studies provide a definitive diagnosis. The objective is to demonstrate the truncal anatomy, type of truncus, status of the branch PAs (origin, size, and presence or absence of stenosis), intracardiac anatomy, additional VSDs, aortic arch and other associated defects, and to evaluate the truncal valve and its function. The echocardiographic features of truncus arteriosus are: (1) one great artery (truncus) originating from the ventricles; (2) a VSD in the conal ventricular septum; (3) overriding of the ventricular septum by the truncal valve; and (4) the PAs arise from the truncus[28-30]. These features are best demonstrated in parasternal long [Figures 37A and 38] and short [Figure 37B] axis, apical four chamber [Figure 39], and sub-costal views.

Thorough evaluation of the PAs, classifying the truncus into different types, namely, I, II or III based on where the PAs arise and how they divide, is of paramount importance. High parasternal short axis [Figure 40] and suprasternal [Figure 41] and tilted subcostal [Figures 42 and 43] views with the use of both 2D echo and color Doppler may help image the origin and branching of the PAs.

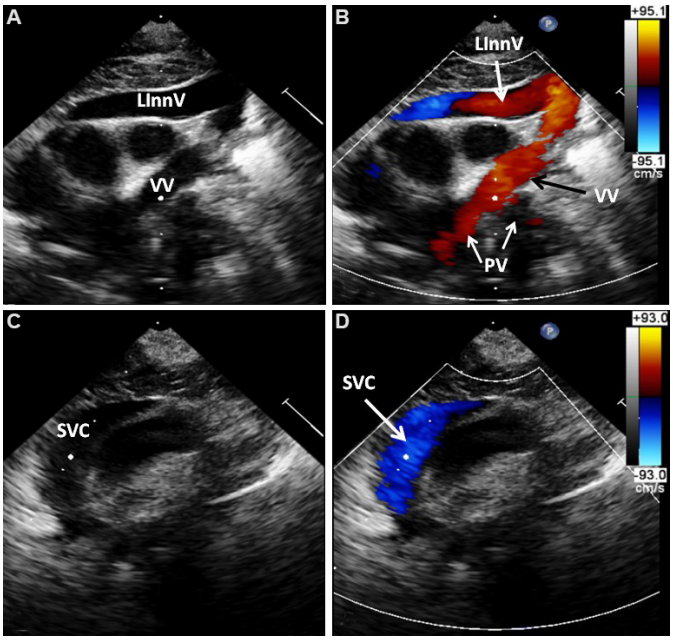

Figure 33. Selected video frames from suprasternal notch views in a neonate with the supra-diaphragmatic type of total anomalous pulmonary venous connection showing a vertical vein (VV), left innominate vein (L Inn), and superior vena cava (SVC); 2-dimensional (A, C) and color flow mapping (B, D) images are shown. Pulmonary veins (PV) draining into the VV are shown in B. Reproduced from Ref.[24].

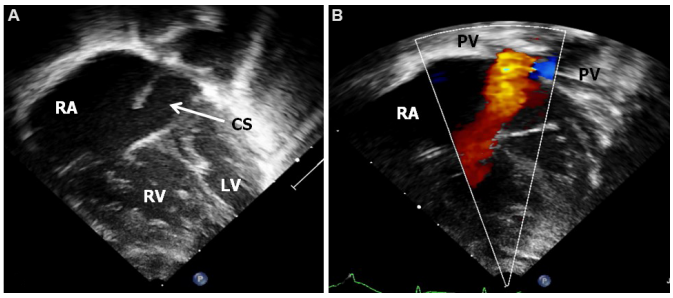

Figure 34. Two-dimensional (A) and color flow mapping (B) images in a patient with a total anomalous pulmonary venous connection to the coronary sinus (CS) demonstrating a dilated CS in 2D (A) and color (B). The pulmonary veins (PV) seem to connect to the CS (B). Reproduced from Ref.[24]. LV: Left ventricle; RA: right atrium; RV: right ventricle.

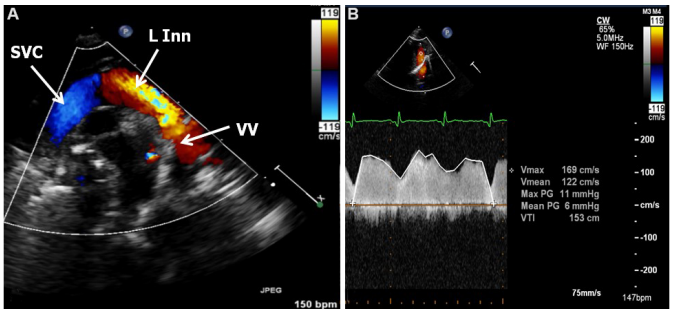

Figure 35. (A) Selected video frame from suprasternal notch view in a neonate with the supra-diaphragmatic type of total anomalous pulmonary venous connection showing a dilated vertical vein (VV), left innominate vein (L Inn), and superior vena cava (SVC). (B) Continuous wave Doppler recordings from the VV show an increased Doppler flow velocity indicative of a mean gradient of 6 mmHg suggestive of obstruction. CW: Continuous wave; PG: peak gradient; VTI: velocity time integral. Reproduced from Ref.[24].

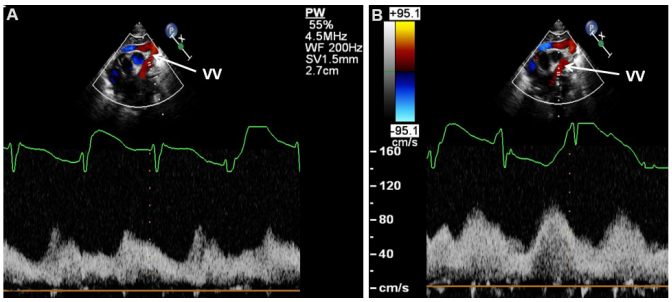

Figure 36. Selected video frames from suprasternal notch view in a neonate with the supra-diaphragmatic type of total anomalous pulmonary venous connection with pulsed Doppler recording form two different portions (A, B) of the vertical vein (VV); the Doppler velocities are low, suggesting that there is no obstruction. Reproduced from Ref.[24]. PW: Pulse width; SV: sample volume; WF: width frequency.

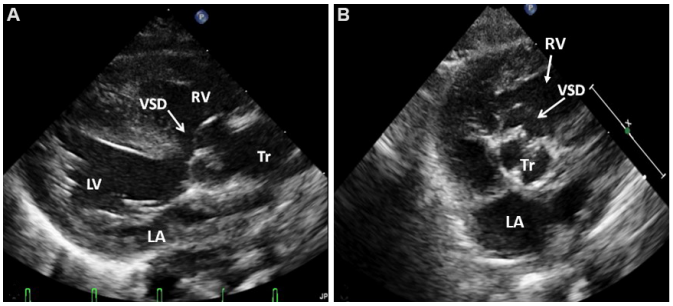

Figure 37. Selected video frames from parasternal long (A) and short (B) axis views showing the truncus (Tr) overriding the ventricular septum and ventricular septal defect (VSD) (arrows). The position of the VSD (arrow) in the conal septum is demonstrated in (B). In (A), the left ventricle (LV) is posterior while the right ventricle (RV) is anterior. In (B), the left atrium (LA) is posterior and the RV is anterior. Reproduced from Ref.[28].

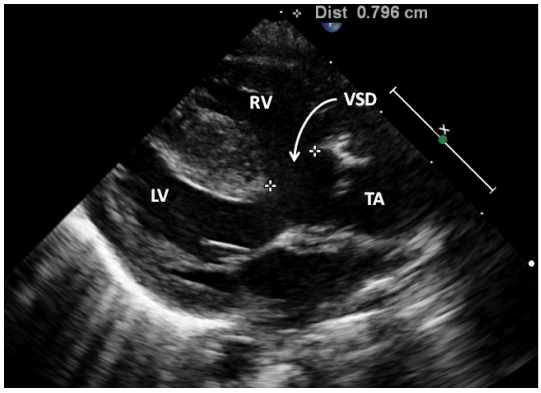

Figure 38. A parasternal long-axis view showing a truncus arteriosus (TA), a ventricular septal defect (VSD) (arrow) and a truncal valve overriding the ventricular septum. The VSD is large and measures approximately 8 mm (insert, Dist). Reproduced from Ref.[30]. LV: Left ventricle; RV: right ventricle.

Pulsed and CW Doppler flow velocities across the branch PAs should be recorded in an attempt to detect stenosis of these vessels. Detection of associated abnormalities, namely, interruption of the aortic arch, variations of the origination of the aortic arch branches, coronary artery origin abnormalities, persistent left superior vena cava, and other VSDs is also feasible by echo-Doppler studies. The presence of narrowing or insufficiency of the truncal valve and branch PA obstructive lesions may also be identified by echo-Doppler

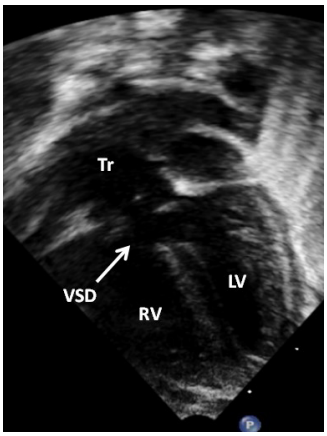

Figure 39. An apical four-chamber view showing the truncus (Tr) overriding the ventricular septum and ventricular septal defect (VSD) (arrow). Reproduced from Ref.[28]. LV: Left ventricle; RV: right ventricle.

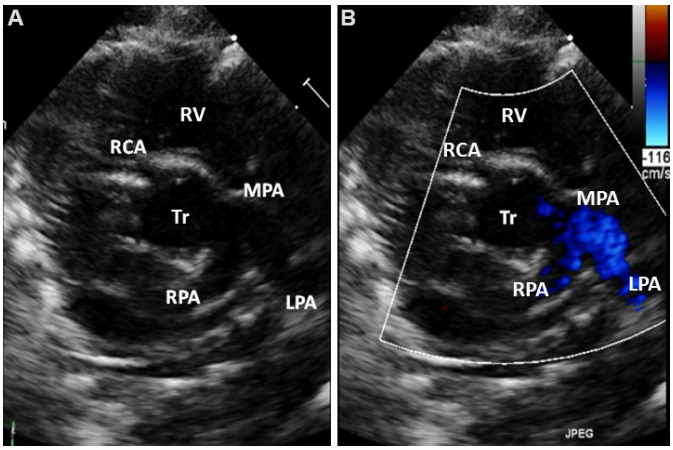

Figure 40. Parasternal short-axis views in 2D (A) and color Doppler (B) showing the origin of the main pulmonary artery from the truncus (Tr). The main pulmonary artery (MPA) is short and bifurcates into the right (RPA) and left (LPA) pulmonary arteries. In (B), color Doppler imaging shows non-turbulent flow in both pulmonary arteries. The Tr is in the middle in both (A) & (B). The MPA, RPA and LPA are shown in color in (B). Reproduced from Ref.[28]. RCA: Right coronary artery; RV: right ventricle.

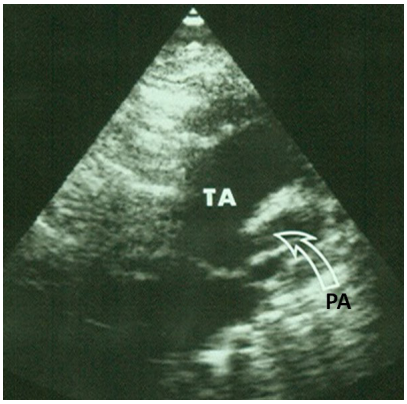

Figure 41. A selected video frame from suprasternal notch view demonstrating the origin of the pulmonary artery (PA) (arrow) from the truncus arteriosus (TA). The branching of the PA is not discerned in this image. Reproduced from Ref.[22].

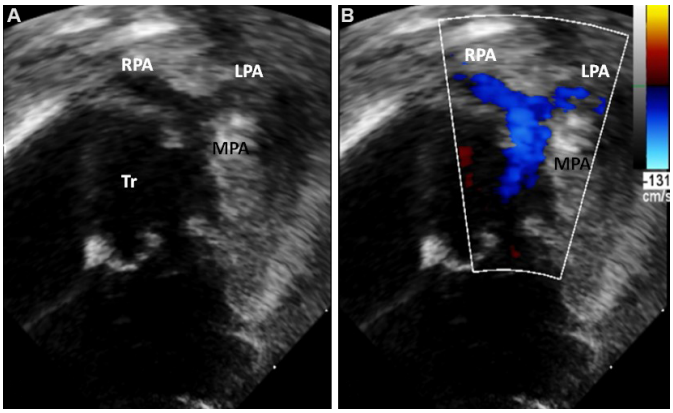

Figure 42. Apical four chamber views [2D (A) and color Doppler (B)] with an anterior tilt of the transducer demonstrating the main pulmonary artery (MPA) originating from the left side of the truncus (Tr). The MPA bifurcates into the right (RPA) and left (LPA) pulmonary arteries. Reproduced from Ref.[28].

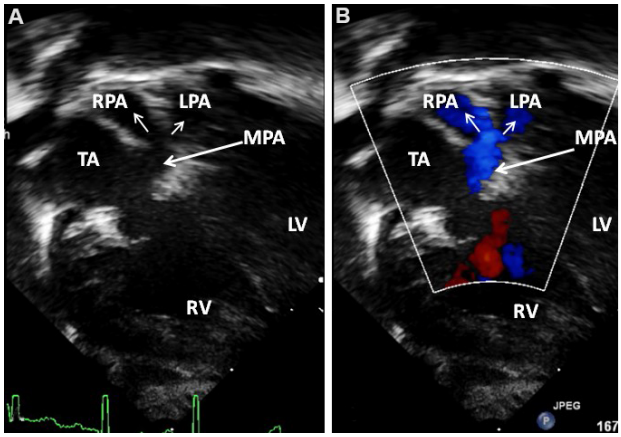

Figure 43. A subcostal coronal view with dual frames, consisting of 2D (A) and color Doppler (B) images. These images demonstrate the main pulmonary artery (MPA) originating from the left side of the ascending portion of the truncus arteriosus (TA) and bifurcating into the right (RPA) and left (LPA) pulmonary arteries. Reproduced from Ref.[30]. RV: Right ventricle; LV: left ventricle.

study. The common truncus must be distinguished from aortopulmonary window and VSD with pulmonary atresia.

Because the diagnosis may be established without any difficulty using echo, angiography is not generally needed to confirm the diagnosis. Rarely, catheterization studies with angiography may be required to define items that were not clearly imaged by echo-Doppler interrogation.

HYPOPLASTIC LEFT HEART SYNDROME

The term, hypoplastic left heart syndrome (HLHS) was initially proposed by Noonan and Nadas[32], who enumerated a number of heart anomalies typified by severe underdevelopment of the LV and proximal aorta. The stated prevalence of HLHS is between 0.21 and 0.28 per 1000 live-born babies, constituting 1.2% to 1.5% of all CHDs. In the severest type, there is atresia of both the aortic valve and mitral valve with a very small proximal aorta and severely hypoplastic LV[22,33-37]. The LA is usually smaller than normal; however, all pulmonary veins drain into it. The mitral valve may be severely stenotic, hypoplastic and even atretic. In patients with mitral atresia, the LV is typically a tiny cavity with thickened LV musculature. In cases with an

open mitral valve, the LV diameter is minute. Fibroelastosis of the endocardium is frequently seen. Stenosis of the aortic valve is present or it is atretic. The ascending portion of the aorta is frequently hypoplastic and its diameter may be between 2 and 3 mm and serves as a channel to perfuse the coronary arterial system retrogradely. Aortic coarctation is seen in a large percentage of cases with this anomaly; however, an interrupted aortic arch is uncommon. The right side of the heart, namely, RA, RV, and PAs, are markedly dilated. A PFO with a left to right shunting is commonly present. Sometimes, it is small and restrictive. On rare occasions, the PFO is fully closed (intact atrial septum). VSD is not usually seen, and it is generally thought to be not an important part of HLHS; however, it has been found in patients with mitral valve atresia with normal aortic root. PDA is seen immediately following birth; however, it is likely to constrict as the baby ages. Markedly hypoplastic LV can be seen in babies with DORV and unbalanced AV septal defect (AVSD); such variants constitute nearly 25% of all hypoplastic left hearts.

Echocardiographic features of HLHS are hypoplasia of the LV [Figures 44-46] and ascending aorta [Figures 44 and 47]. In addition, there may be hypoplasia, stenosis or atresia of either the aortic [Figures 44 and 47] and/or mitral [Figure 45] valves. The LA is generally small [Figures 44 and 45].

The RA, RV [Figures 44-48], and main PA [Figures 44, 48 and 49] are dilated and are easily seen on 2D imaging. The degree of patency of the PDA should be assessed [Figures 49]. Evaluation of the arch of the aorta and descending aorta should be undertaken to confirm or exclude coarctation of the aorta.

Hemodynamic information may be appraised by a combination of pulsed and CW Doppler and color flow imaging. Doppler examination of the transverse aortic arch reveals retrograde flow [Figures 50 and 51], which identifies systemic circulation that is ductal dependent and that the LV is not adequate for going with a biventricular type of repair. High Doppler velocity through the PFO indicates restriction of the inter-atrial defect [Figure 52].

The dimension of the LV differs from one patient to the next, as shown in [Figures 53 and 54]; but all of them have similar physiology and require the same type of Norwood palliation. Similarly, the diameters of the ascending aorta also vary [Figure 55], and again all these patients require similar Norwood surgery, but some studies indicate a very small ascending aorta (< 1 mm) may put them at an increased risk for poor prognosis after the Norwood palliation.

DOUBLE-OUTLET RIGHT VENTRICLE

DORV is an uncommon CHD; in this anomaly, both the PA and aorta originate from the morphological RV[22,38,39] and comprise close to 1% of all congenital cardiac defects. Several definitions to describe this anomaly have been proposed; most common of these are: (1) both great vessels arise from the RV and none of the great vessels have fibrous continuity with the AV valves; and (2) one whole great artery and larger than one-half of the remaining great artery come off of the RV. A large VSD is typically seen and is the only exit from the LV. The size and location of the VSD establish the pathophysiology. In the most common type, the ventricular defect is perimembranous and sub-aortic in location, directing the LV blood into the aorta and this type constitutes 50% of all DORV cases. In the absence of PS, the clinical features are akin to those of the usual VSD. In patients with significant PS, the clinical presentation is similar to those of tetralogy. In cases with the VSD in the sub-pulmonary region, the LV output is mostly directed into the PA; this will result in physiology similar to that of TGA, and such a defect is commonly called as Taussig-Bing malformation. This variety comprises 25% of all DORV cases. In the leftover 25% of patients, the ventricular defect is either non-aligned with either great artery or is doubly committed equally to both arteries[22,38,39]. The VSD is typically large; however, it may be absent in very rare cases causing LV hypoplasia. In some

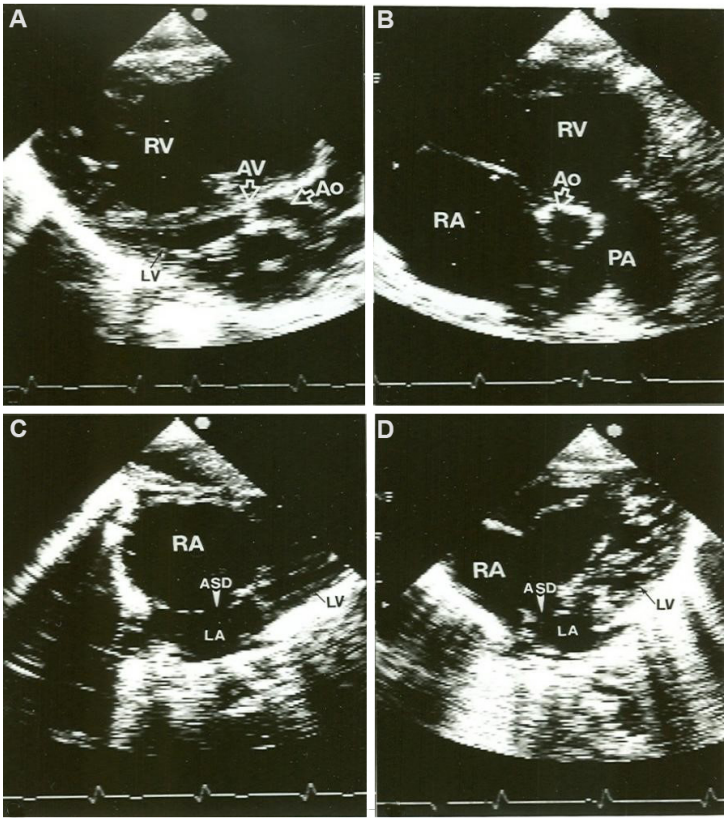

Figure 44. Selected video frames from a two-dimensional echocardiographic study in a neonate with hypoplastic left heart syndrome demonstrating: (A) a very small left ventricle (LV), severely stenotic aortic valve (AV) and a small aorta (Ao). Note the large right ventricle (RV). (B) short-axis view demonstrating a small Ao, large right atrium (RA), RV and pulmonary artery (PA). (C) Subcostal view showing a large RA, small left atrium (LA) and a small LV. The atrial defect (ASD) is shown with an arrowhead. (D) Another subcostal view, again demonstrated large RA, small LA, small LV and a large RV (not labeled), and an ASD (Arrowhead). Reproduced from Ref.[21].

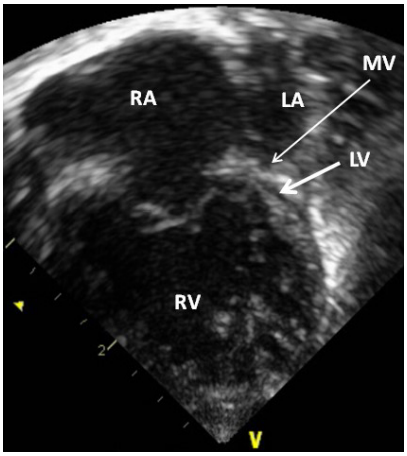

Figure 45. A selected video frame from a 2D echocardiographic apical four-chamber view in a neonate with hypoplastic left heart syndrome, showing a markedly hypoplastic, slit-like (thick arrow) left ventricle (LV), a markedly enlarged and hypertrophied right ventricle (RV), and an enlarged right atrium (RA). The atretic mitral valve (MV) (thin arrow) and hypoplastic left atrium (LA) are also shown. Reproduced from Ref.[21].

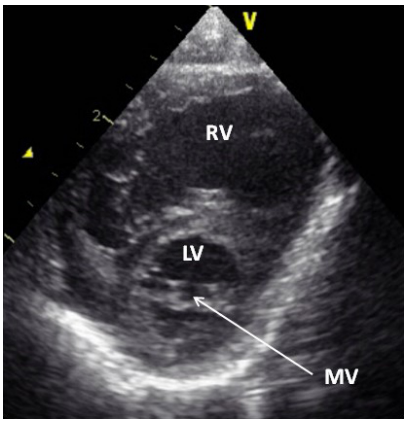

Figure 46. A selected frame from a 2D echocardiographic parasternal short-axis view in another neonate with hypoplastic left heart syndrome demonstrates a small left ventricle (LV) and a large right ventricle (RV). A very small mitral valve (MV) (arrow) is also shown. Reproduced from Ref.[21].

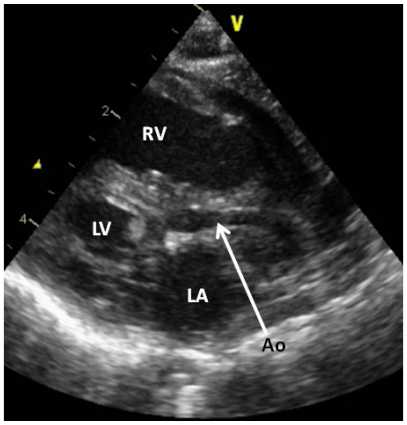

Figure 47. A selected frame from a 2D echocardiographic parasternal long-axis view of a neonate with hypoplastic left heart syndrome demonstrates a small left ventricle (LV), a markedly hypoplastic aorta (Ao) (arrow), and a large right ventricle (RV). Reproduced from Ref.[21]. LA: Left atrium.

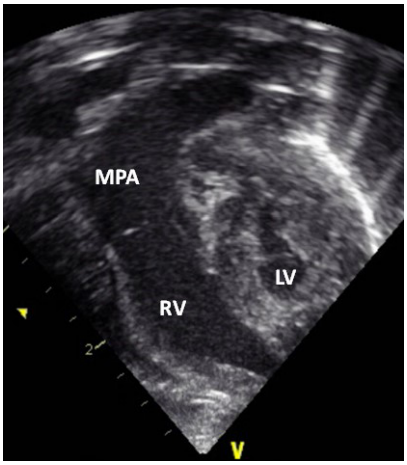

Figure 48. A selected video frame from a 2D echocardiographic apical four-chamber view in a neonate with hypoplastic left heart syndrome, showing a hypoplastic left ventricle (LV) and markedly enlarged right ventricle (RV) and main pulmonary artery (MPA). Reproduced from Ref.[21].

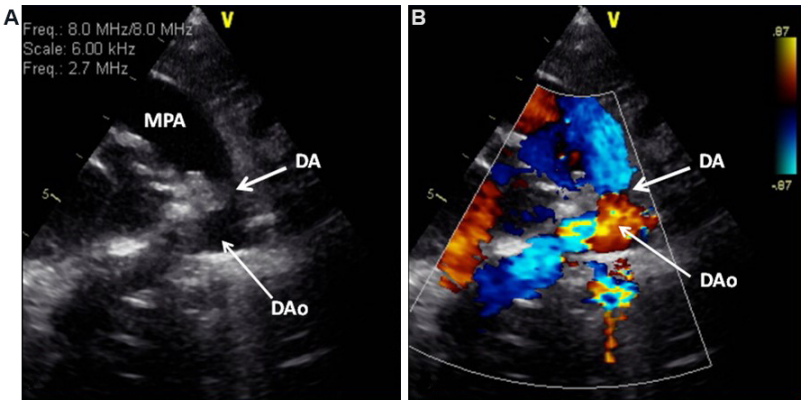

Figure 49. A selected video frame from 2D (A) and color Doppler (B) parasternal short-axis view in a neonate with hypoplastic left heart syndrome demonstrating a somewhat constricted ductus arteriosus (DA) prior to the administration of prostaglandin E_1. Reproduced from Ref.[21]. DAo: Descending aorta; MPA: main pulmonary artery.

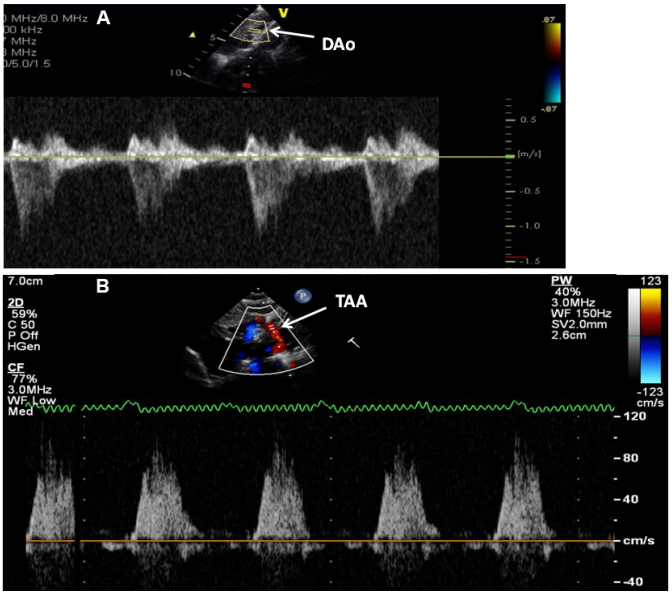

Figure 50. Doppler interrogation of the descending aorta (DAo) (A) and transverse aortic arch (TAA) (B) showing forward flow in the DAo and retrograde systolic flow in TAA; the latter finding indicates ductal-dependent systemic circulation. Reproduced from Ref.[21].

patients with initially large VSDs, the defects decrease in size spontaneously following birth with resultant marked LV outflow obstruction[40-42]. The PS is frequently at valvar or subvalvular level; atresia of the pulmonary valve/artery may be seen rarely. In cases with a sub-pulmonary VSD, subaortic stenosis may be seen and such patients may also have aortic coarctation. The great arteries are not normally related in most subjects: two-thirds of the patients have side-by-side relationships, 25% have d-malposition, and a small minority have l-malposition. A normal great artery relationship is observed mainly in subjects with a sub-aortic VSD.

Echocardiography is valuable in the assessment of the diameter and function of both LV and RV, the diameter and position of the VSD, and the great artery relationship [Figures 56 and 57]. The degree of PS may be quantified with Doppler studies. Subaortic stenosis and aortic coarctation should be searched for in babies with sub-pulmonary VSDs. Catheterization studies are usually not required because

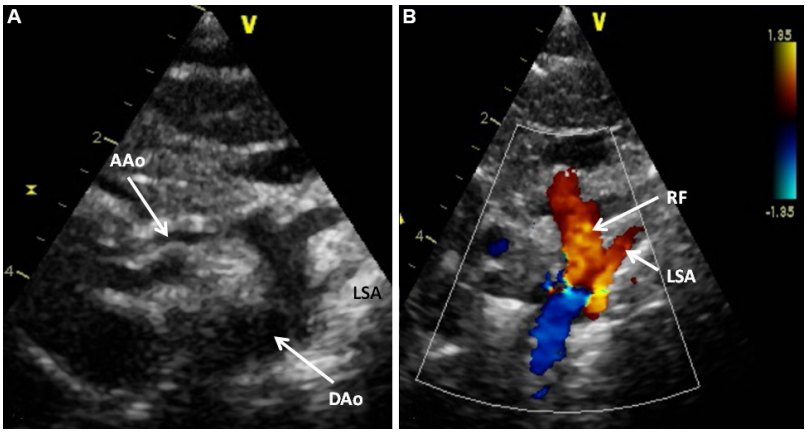

Figure 51. A selected video frame from 2D (A) and color Doppler (B) suprasternal notch views of the aortic arch in a neonate with hypoplastic left heart syndrome. A markedly hypoplastic ascending aorta (AAo) is shown and serves only to deliver blood in a retrograde fashion to the coronary arteries. Retrograde flow (RF) in the arch of the aorta (B) suggests a ductal-dependent systemic circulation. Reproduced from Ref.[21]. DAo: Descending aorta; LSA: left subclavian artery.

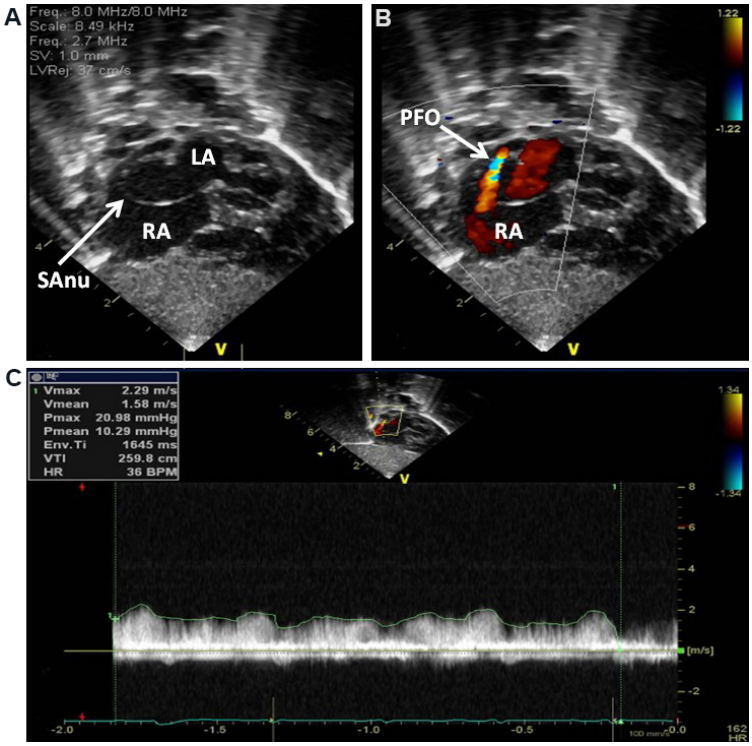

Figure 52. Selected video frames from subcostal views of the atrial septum in a neonate with hypoplastic left heart syndrome demonstrating a septal aneurysm (SAnu) (A, B), turbulent flow across the patent foramen ovale (PFO) (arrow in B), and a high-velocity flow across the PFO (C). A Doppler-estimated gradient over 10 mmHg (insert in C) and turbulent flow (B) suggest a restrictive PFO. Reproduced from Ref.[21]. LA: Left atrium; RA: right atrium.

echocardiographic studies clearly show anatomy and physiology.

UNIVENTRICULAR HEARTS

The term, univentricular heart, has been applied to characterize any defect with a single functioning

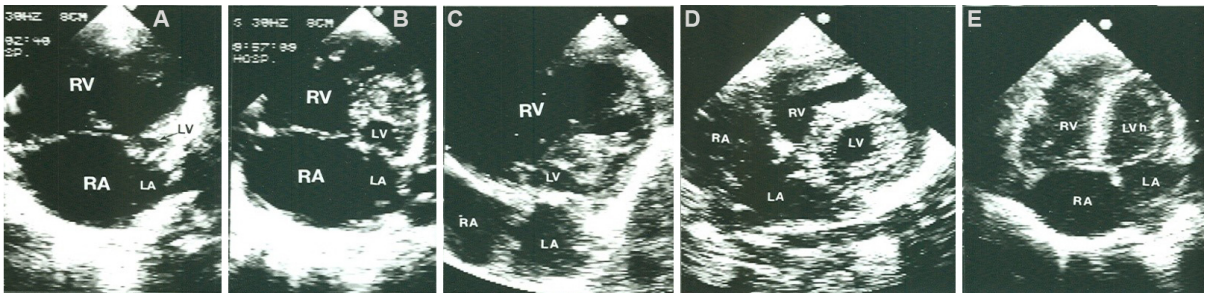

Figure 53. Selected video frames from four-chamber two-dimensional echocardiographic views in five different neonates with varying sizes of the left ventricle (LV) (A-E). Reproduced from Ref.[21]. LA: Left atrium; RA: right atrium; RV: right ventricle.

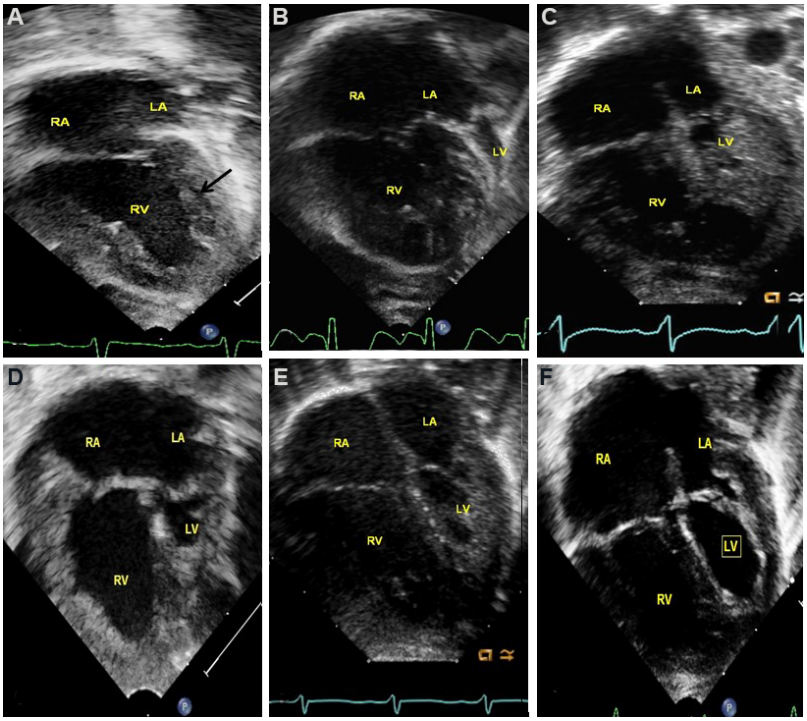

Figure 54. Selected video frames from apical four chamber views of six different babies with hypoplastic left heart syndrome, demonstrating varying degrees of left ventricular (LV) hypoplasia, starting from slit-like LV in (A) (arrow), and progressively larger LVs in (B-F). All of them require Norwood palliation. Other features shown are a small left atrium (LA), large right atrium (RA), and large right ventricle (RV). Reproduced from Ref.[36].

ventricular chamber. Such defects include single ventricle, common ventricle, double-inlet left ventricle (DILV), and univentricular AV connection[22,39]. These variants account for less than 2% of all CHDs. In such hearts, it may be that both of the AV valves empty into the single ventricle, i.e., DILV, only one AV valve empties into the single ventricular chamber (with atresia of the other AV valve), or that a single (common) AV valve empties into the ventricular chamber. DILV is the most frequent among the univentricular hearts and will be reviewed in this section. In cases with DILV, the ventricular chamber most commonly has the morphology of LV; however, RV, mixed, indeterminate, or undifferentiated morphological variants were observed in the past. The main ventricle is principally a morphologic LV with an outlet chamber coupled to it; the outlet chamber has a morphology of RV. Both the AV valves may be normally formed. Or, one of the AV valves may have hypoplasia, stenosis, or even atresia. The great vessels most commonly have transposition with the aortic origin from the hypoplastic RV, and the PA origin from

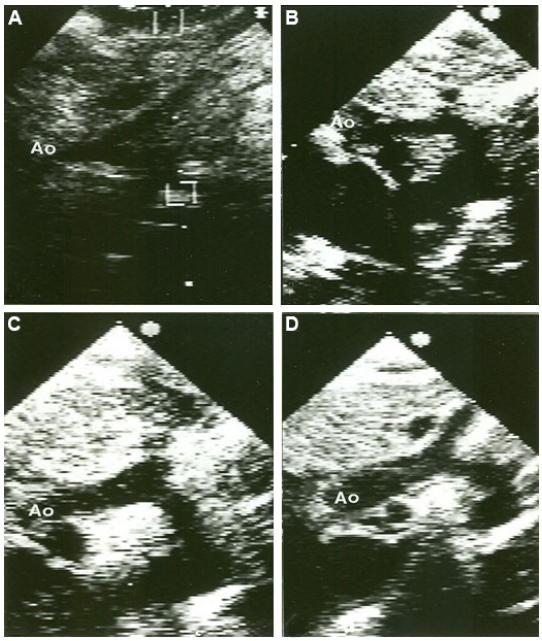

Figure 55. Selected video frames from suprasternal notch views of four different babies (A-D) with hypoplastic left heart syndrome, demonstrating varying degrees of ascending aortic (Ao) hypoplasia. Reproduced from Ref.[37].

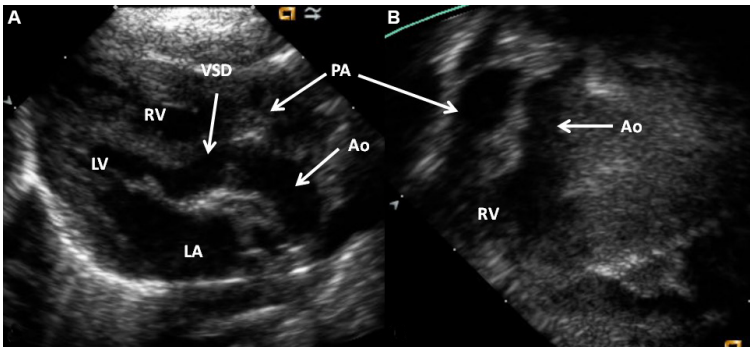

Figure 56. Selected video frames from the parasternal long-axis (A) and subcostal four chamber (B) views of a patient with double-outlet right ventricle and normally related great arteries, demonstrating the origin of both the aorta (Ao) and the pulmonary artery (PA) from the right ventricle (RV). The ventricular septal defect (VSD) is shown. The vessel labeled as PA was shown to divide into right and left PAs, but not shown in the echo images. Reproduced from Ref.[39]. LA: Left atrium; LV: left ventricle.

the main LV cavity. L-TGA occurs more frequently than d-TGA. The great arteries are related in a normal fashion in less than 30% of patients. DORV is also seen where both great arteries take origin from the smallish RV. PS is seen in 2/3rds of cases and PS is present regardless of the great vessel alignment. The narrowing may involve the valvular or sub-valvular components. Or, there may be atresia of the pulmonary valve/artery. Obstruction at the subaortic level may be seen in patients with TGA and is secondary to the small VSD (bulbo-ventricular foramen). Subjects with subaortic narrowing frequently have accompanying aortic coarctation.

Echocardiography is helpful in establishing the diagnosis. The lack of the interventricular septum is easily shown [Figure 58]. The AV valves [Figure 58] and their attachment to the ventricle [Figures 58 and 59], ventricle to great artery relationship, and the existence of PS [Figure 59] may be determined by echo-

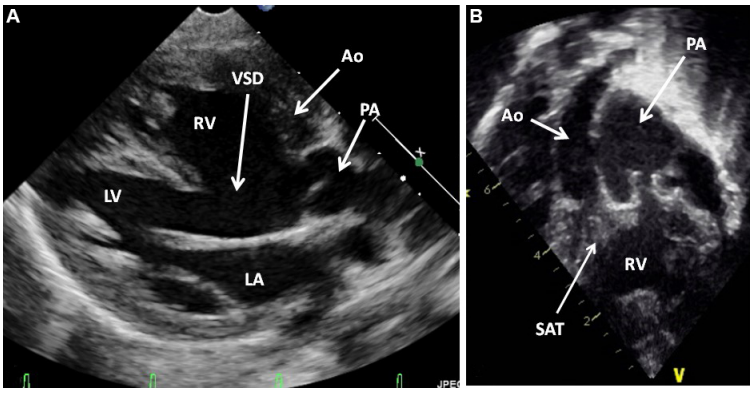

Figure 57. Selected video frames from the parasternal long-axis (A) and subcostal (B) views of another patient with double-outlet right ventricle and transposed great arteries (Taussig-Bing), demonstrating the origin of both the aorta (Ao) and the pulmonary artery (PA) from the right ventricle (RV). An extremely large ventricular septal defect (VSD) is also shown. Reproduced from Ref.[39]. LA: Left atrium; LV: left ventricle; SAT: subaortic tissue.

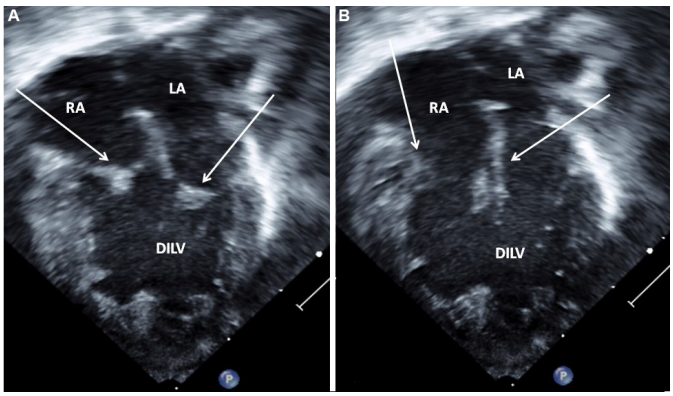

Figure 58. Selected video frames from apical four-chamber views of a patient with double inlet left ventricle (DILV) with closed (A) and open (B) atrioventricular valves (arrows) during ventricular systole and diastole, respectively. The outlet chamber is not visualized in this view (see Figure 59). Reproduced from Ref.[39]. LA: Left atrium; RA: right atrium.

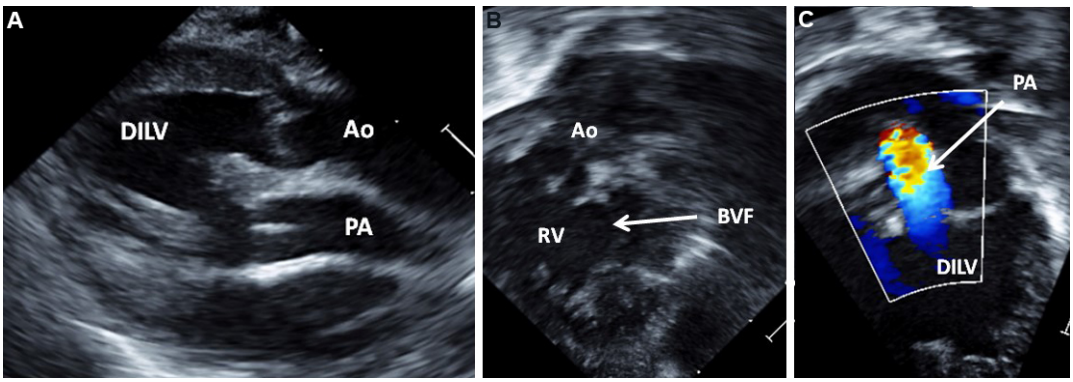

Figure 59. Selected video frames from the parasternal long-axis (A) and modified apical (B, C) views of the same patient as is shown in [Figure 58], demonstrating transposition of the great arteries (A) with the aorta (Ao) anteriorly and pulmonary artery (PA) posteriorly. The connection of the right ventricle (RV) (outlet chamber) with the main chamber by a bulbo-ventricular foramen (BVF) is shown in the (B). This chamber gives rise to the aorta (Ao), as seen in the (B). The origin of the PA from the main chamber [double-inlet left ventricle (DILV)] is shown in the (C). Note the turbulent flow in the PA (C), suggesting stenosis. Continuous wave Doppler across this region (not shown) revealed high velocity suggestive of significant pulmonary stenosis. Reproduced from Ref.[39].

Doppler studies. Doppler flow velocity recordings across the pulmonary and sub-pulmonary region will help assess the degree of PS. In subjects with transposition, the dimension of the bulbo-ventricular foramen and evidence for obstruction across it should be scrutinized. Such obstructions may exist at the time of presentation, develop later during the natural process of growth or may develop following pulmonary artery banding[43]. Aortic coarctation [Figure 27] may be seen in some of these patients.

INTERRUPTED AORTIC ARCH

Aortic arch interruption is characterized as a total absence of luminal communication amongst the ascending and descending portions of the aorta. This is in contradistinction to aortic coarctation, in which there is usually a luminal connection[4,22,44]. This lesion comprises less than 1% of all heart defects. Three forms of the interrupted aortic arch (IAA) have been designated[45]: (1) Type A. The aortic arch interruption is located past the left subclavian artery; (2) Type B. The arch interruption occurs in-between the left common carotid and left subclavian arteries; and (3) Type C. The arch interruption is in-between the right innominate and left common carotid arteries. Type B interruption is the utmost frequent, consisting of 52% of IAA cases. Type A interruption is the next most frequent, accounting for 44% of cases. Type C interruption is least frequent, occurring in only 4% of cases. IAA occurs irrespective of where the aortic arch descends, i.e., left or right. IAA is generally seen with other heart defects. PDA is the most common among these, providing continuousness in-between the PA and the descending portion of the aorta. VSDs are seen in nearly 80% of Type B IAA cases while it is present in only 50% of babies with Type A interruption. Valvar and subvalvular aortic stenosis, truncus arteriosus, DORV of the Taussig-Bing type, single ventricle (DILV), TGA, and aorto-pulmonary window are also seen in patients with IAA. A strong connection with DiGeorge's syndrome (chromosome 22q11 microdeletion) has been observed, particularly with Type B interruption.

Two-dimensional echocardiographic and color Doppler studies from supra-sternal notch view[46] usually confirm [Figure 60] the diagnosis. MRI studies and angiography are not usually necessary to establish a diagnosis.

Because of high association with VSD, a careful review of parasternal, apical and subcostal views should be undertaken to assess the size, location and shunt across the VSD. Since valvar and subvalvular aortic stenosis, truncus arteriosus, DORV of the Taussig-Bing type, DILV, TGA, and aorto-pulmonary window are observed in subjects with IAA; these defects should be excluded during the echo-Doppler study.

PULMONARY ATRESIA WITH INTACT VENTRICULAR SEPTUM

Pulmonary atresia with the intact ventricular septum (IVS) is a severe cyanotic CHD typified by complete obstruction of the pulmonary valve, two distinct ventricles, a patent tricuspid valve, and no ventricular defect[4,22,47-50]. It is an uncommon disorder, present in 1% of all CHDs. The RV is typically hypoplastic with varying RV sizes. The main PA, as well as PA branches are frequently normal in diameter; this is in contrast to VSD with pulmonary atresia, in which the PAs are generally smallish with hypoplasia. A PFO is seen in almost all patients, allowing right to left shunt, helping to decompress the RA. Arteriovenous fistulae of the coronary arteries may be found in 10% to 50% of infants. A few of these cases may have coronary circulation dependent on high RV pressure; these babies do not tolerate relieving of obstructive components of the RV.

The blood return from the systemic veins to the RA requires satisfactory egress. Because of an IVS, the only exit for the RA blood is across an atrial defect. An adequately sized PFO or ASD is critical for RA decompression. The desaturated blood from the RA traverses through the PFO/ASD into the LA and combines with the fully oxygenated blood from the pulmonary veins, producing central cyanosis. The PDA

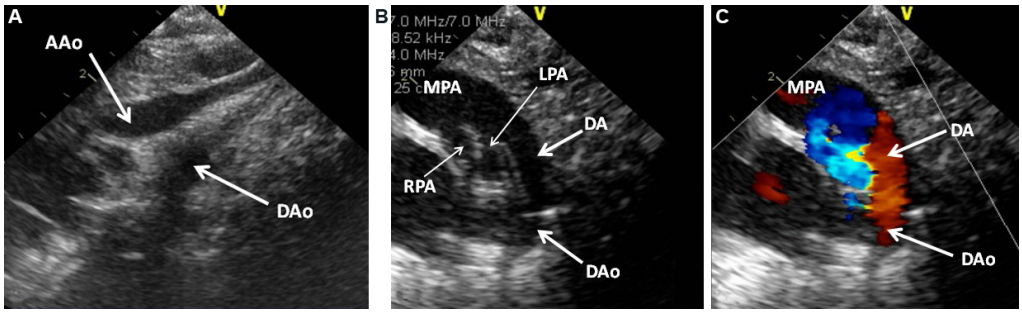

Figure 60. Selected video frames from supra-sternal notch (A) and high parasternal short axis (B, C) views in a neonate with interrupted aortic arch. (A) The ascending (AAo) and descending (DAo) aortas are seen without any connection between them in this and other views. (B, C) show the ductus arteriosus (DA) connecting the main pulmonary artery (MPA) with the DAo, thus providing blood flow to the lower part of the body. The baby has already been on prostaglandin E_1 infusion. Reproduced from Ref.[39]. LPA: Left pulmonary artery; RPA: right pulmonary artery.

is the lone supply of pulmonary blood flow, although aorto-pulmonary collateral vessels may on rare occasions provide such flow. The size of the PDA, the extent of flow through it, and the status of PA pressure and resistance will determine the clinical presentation and course in the early newborn period.

Two-dimensional echocardiography is diagnostic; it will show a small RV without forwarding blood flow from the RV across the pulmonary valve into the PAs. Tricuspid valve insufficiency is seen in most patients. Tricuspid valve annulus Z scores are chiefly predictive of the RV's potential growth; therefore, the annulus should be carefully measured. RA to LA shunt via the PFO and aorta to PA shunt through the PDA are shown by pulsed and color Doppler. Catheterization with angiography is not generally needed for making a diagnosis, but is necessary if percutaneous intervention to open up the pulmonary valve[48,50] is contemplated. Following confirmation of the diagnosis, several measurements, namely, sizes of the tricuspid valve (Z score), RV, pulmonary valve annulus, and PAs are also made. Color Doppler imaging of the RV wall may offer evidence regarding coronary sinusoids. Some of these features are illustrated in [Figures 61 and 62].

CONGENITAL CORRECTED TGA

Congenital corrected TGA is a rare complex CHD. In the most common form, the atria are normally positioned (atrial situs solitus), AV discordance is present, the morphological LV (MLV) is to the right and the morphological RV (MRV) is to the left, and ventriculo-arterial discordance exists. In essence, the ventricles are inverted. The RA passes the systemic venous return into a morphological LV on the right, and then into the PA. The LA empties the pulmonary venous blood into a morphological RV on the left, and then into the aorta; thus, the blood circulation is normal[39,51-53]. Because the aorta comes off the RV and the PA arises from the LV, transposition of great vessels is deemed to be present. However, the blood flow pattern is normal, hence the term congenitally corrected TGA (CCTGA), or corrected transposition for short. Normally the aortic valve is positioned onto the right side of the pulmonary valve; however, in this defect, the aorta is located to the left of the PA; therefore, the designation of l-TGA. The incidence of this defect is close to 0.5% of all CHDs[54].

An echocardiogram is diagnostic, although it may be a challenge for the beginner to perform and interpret. Lack of continuity in-between the left AV valve and the aortic valve secondary to a conus on the left side is one of the echo features. Scrutiny of the AV valve attachment may help diagnose ventricular inversion; a higher level of mitral valve leaflet attachment on the right side compared to the attachment of the tricuspid valve leaflet on the left side indicates that the ventricles are inverted [Figure 63].

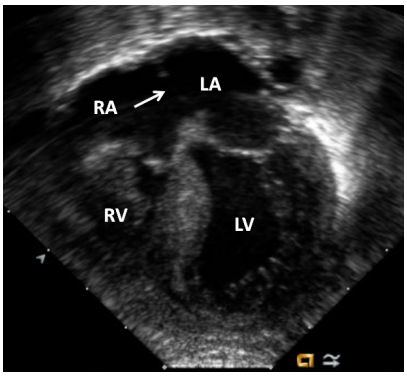

Figure 61. An echocardiogram (apical 4-chamber view) of an infant with pulmonary atresia with an intact ventricular septum. Severe tricuspid valve hypoplasia with a severely hypoplastic right ventricle (RV) and a thick myocardium is seen. An arrow indicates the location of an atrial defect. Subsequent imaging with color Doppler showed random color signals in the RV myocardium, raising suspicion of coronary sinusoids. This was confirmed by the angiogram performed later. Reproduced from Ref.[50]. LA: Left atrium; LV: left ventricle; RA: right atrium.

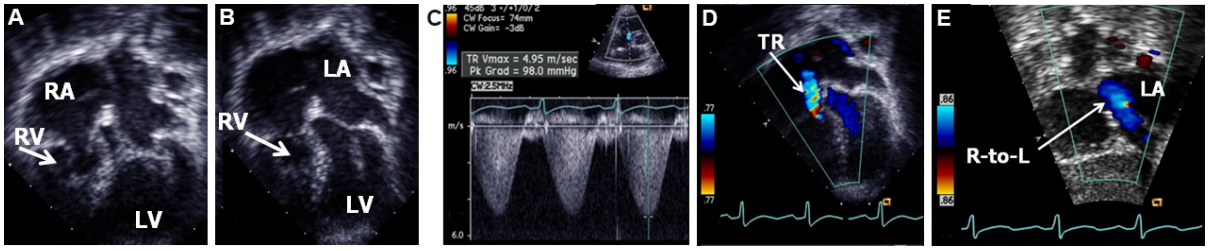

Figure 62. Selected video frames from 2D (A, B), continuous wave (C), and color (D, E) Doppler images, demonstrating a very small/hypoplastic right ventricle (RV) with open (A) and closed (B) tricuspid and mitral valve leaflets (not marked) in apical four chamber (A, B) views during ventricular diastole and systole, respectively. A high tricuspid regurgitation Doppler velocity (C) indicative of high RV pressure, tricuspid regurgitation (TR) (D), and a right-to-left (R-to-L) shunt across the patent foramen ovale (E) are shown. The pulmonary artery is supplied by the ductus (not shown). Reproduced from Ref.[45]. LA: Left atrium; RA: right atrium; LV: left ventricle.

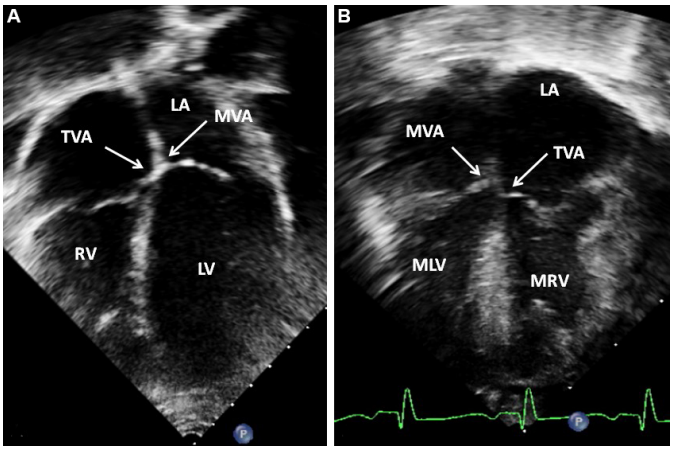

Figure 63. Selected video frames from apical four-chamber echocardiographic views of two infants. (A) A normal ventricular relationship; note the higher level of attachment of the mitral valve (MVA) compared to the tricuspid valve attachment (TVA). (B) Ventricular inversion; note the higher level of attachment of the mitral valve (MVA) on the right compared to the tricuspid valve attachment (TVA) on the left, indicating that the ventricles are inverted. Reproduced from Ref.[39]. LA: Left atrium; LV: left ventricle; MLV: morphologic left ventricle; MRV: morphologic right ventricle; RA: right atrium; RV: right ventricle.

Although patients with no other heart defects have been reported, the majority of CCTGA cases have other significant heart defects, namely, VSD, right-sided MLV outflow tract narrowing, atrio-ventricular block (spontaneous or after catheter or surgical intervention) and an Ebstein's type of abnormality of the morphologic tricuspid valve on the left-side[55]. The right-sided MLV outflow tract narrowing is seen in 44% to 57% of cases[52]. More common causes of such obstruction are pulmonary valve atresia, valvar PS, and sub-pulmonary stenosis secondary to muscular mal-alignment and/or hypertrophy. Less frequently seen reasons are accessory valve tissue, fibrous tags, membranous septal aneurysms, and intra-cardiac blood cysts[52].

The amount of downward dislocation of the left-sided tricuspid valve is assessed in a four-chamber view [Figure 64]. The size, location and shunting across the VSD should be demonstrated. The degree of PS may be quantified by Doppler studies using the modified Bernoulli equation.

Echocardiographic examples of ventricular septal aneurysms causing obstruction to MLV both in cases with levocardia [Figure 65][52] and dextrocardia [Figures 66 and 67][56] are shown.

EBSTEIN'S ANOMALY OF THE TRICUSPID VALVE

Ebstein's malformation of the tricuspid valve is a CHD comprising downward (towards the apex of the heart) displacement of septal and posterior leaflets of the tricuspid valve[4,51,57-60]. In addition, there are redundant tricuspid valve leaflets and tricuspid valve apparatus dysplasia, producing regurgitation and infrequent stenosis. Varying degrees of downward dislocation of the tricuspid valve attachment from a few mm to all the way close to the parietal band and crista supraventricularis have been reported. The RV inflow portion from the true to false annuli of the tricuspid valve is named atrialized RV and forms a common compartment with the RA. Severe RA dilatation is also present. Pulmonary atresia or stenosis may be seen in some cases. Ebstein's malformation of the tricuspid valve is an uncommon congenital cardiac defect comprising 0.3% to 0.6% of all CHDs.

The pathophysiology is variable and is largely related to the extent of downward dislocation of the tricuspid valve leaflets. In subjects with moderate to severe degrees of Ebstinization of the tricuspid valve, RA contraction propels the blood into the atrialized component of the RV, and with each RV contraction, the RV blood is ejected back into the RA; such "ping-pong" effect[51] increases RA pressure, produces RA enlargement resulting in a shunt from RA to LA across the PFO/ASD. In the neonate with high pulmonary vascular resistance (PVR), this effect becomes more pronounced, causing severe cardiomegaly and decreased pulmonary blood flow. As the PVR falls, the infant will have reduced cyanosis. However, this abnormality returns late during childhood and adolescence because of decreased efficiency of the tricuspid valve apparatus. The role of high PVR in the neonate should be recognized while performing and interpreting the echo study by the echocardiographer.

A two-dimensional echocardiogram shows RA enlargement and downward dislodgment of the tricuspid valve leaflets [Figures 68A and 69A]. The anatomy of the leaflets, including valve dysplasia and abnormalities of the chordal attachments, should be evaluated. Doppler studies show tricuspid insufficiency [Figure 68B] and shunting from RA to LA via the PFO [Figure 69B]. Peak tricuspid regurgitation velocity may be used in estimating the RV/PA systolic pressures by the use of a simplified Bernoulli formula. The patency of the ductus should also be evaluated. Even though the atrialized part of the RV bulges into the LV outflow tract [Figure 70], clinically significant LV outflow tract obstruction rarely occurs.

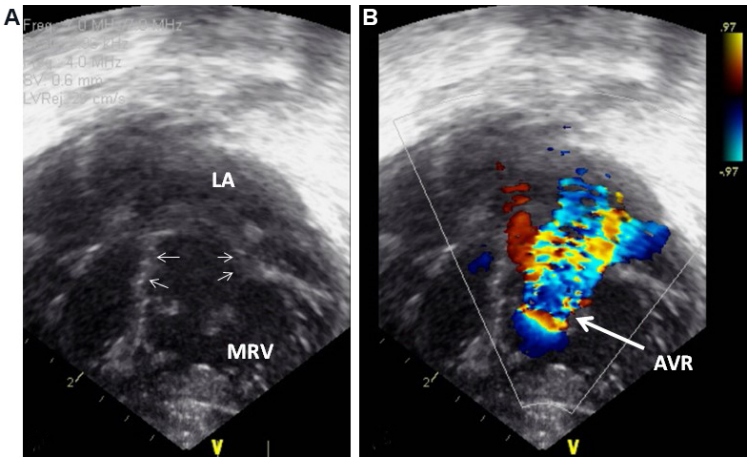

Figure 64. (A) A selected modified apical view demonstrating the downward displacement of a left-sided morphologic tricuspid valve attachment (small arrows) in a neonate with I-TGA. (B) Color flow image of the same infant, showing severe atrioventricular valve regurgitation (AVR). Reproduced from Ref.[39]. LA: Left atrium; MRV: morphologic right ventricle.

Apical four-chamber views of the echocardiogram [Figure 71] may be used to derive the Celermajer index[61]. The index is calculated as follows: ratio of the area of the RA + the atrialized component of the RV to the pooled area of the noninvolved RV, LV and LA [Figure 71]. The higher the grade, the greater is the mortality: (1) Grade 1 (a ratio of < 0.5) - mortality of 0%; (2) Grade 2 (a ratio of 0.5 to 0.99) - mortality of 10%; (3) Grade 3 (a ratio of 1.0 to 1.49) - mortality of 44%; and (4) Grade 4 (a ratio of ≥ 1.5) - 100% mortality[61]. The Celermajer index is also used in the calculation of Simpson-Andrews-Sharland Score[62], which also predicts prognosis.

The pulmonary valve may fail to open adequately, either due to anatomic valve leaflet fusion (true pulmonary valve atresia) or due to functional atresia of the pulmonary valve due to the inability of the RV to generate systolic pressure high enough to overcome the pressure in the PA. The PA pressure may be elevated in the early neonatal period due to high PVR or a large PDA transmitting aortic pressure to the PA. Sometimes it is not easy to distinguish functional type from true atresia of the pulmonary valve, but if a pulmonary insufficiency jet on color Doppler imaging is seen, that would indicate functional type of the pulmonary valve atresia.

MITRAL ATRESIA WITH NORMAL AORTIC ROOT

Mitral valve atresia with normal aortic root is a rare complex heart defect and is frequently seen in association with numerous other abnormalities. The mitral valve atresia may be due to an absence of AV connection or secondary to an imperforate valvar membrane[39,63]. In babies with ventricular inversion, the atretic valve may be a morphologic tricuspid valve, as seen in tricuspid atresia hearts of Type III, subtypes 1 and 5[15]; however, the physiology is that of mitral atresia. For this reason, the use of the term "left AV valve atresia" may be justified. The LA is small and hypoplastic and the RA is dilated and hypertrophied. A PFO/ASD is usually seen; a PFO in two-thirds of cases and an ASD in one-third. An obstructive atrial communication, and rarely, an intact atrial septum may be present. Most commonly, a single ventricle is seen, though in a few patients both ventricles are present. In patients with both ventricles, the LV is hypoplastic and connects with the RV via a small ventricular defect. The RV is always enlarged and hypertrophied. TGA is frequently seen. DORV is present in some babies. In the majority of cases, normal pulmonary valve without stenosis is seen; yet, in 25% to 30% of cases, stenosis at valvar and/or sub valvar level or even atresia may be present. The ascending aorta and aortic valve, by definition, are near normal in

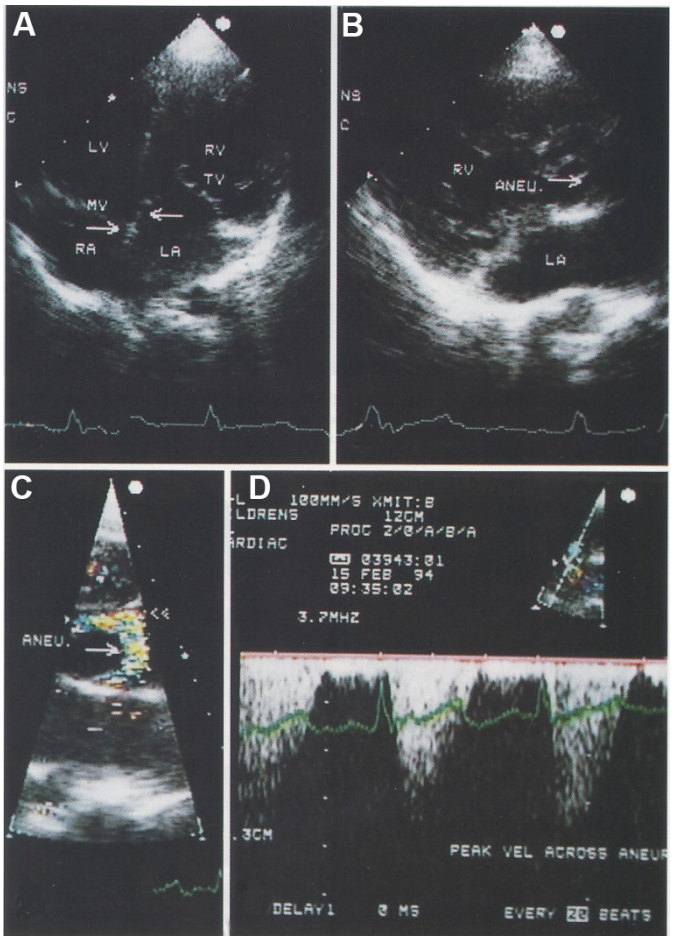

Figure 65. (A) Selected video frame from apical four-chamber view, demonstrating the reversal of the ventricles. In this apical four chamber view, the apex is positioned at the top, the morphologic left ventricle (LV) is placed to the right and the morphologic right ventricle (RV) is shown on the left. The right (RA) and left (LA) atria are shown at the bottom of the Figure. The attachment of the mitral valve (MV) leaflet is higher (arrow on the left) than that of the tricuspid valve (TV), indicating that the morphologic LV is on the right side and the morphologic RV is on the left side. The RA is connected to the morphologic LV and the LA to the morphologic RV. Also, note that the medial leaflet of the TV is plastered onto the ventricular septum (arrow on the right), suggesting Ebstein's type of abnormality of the morphologic TV. (B, C) Selected video frames from a parasternal long-axis view demonstrating an aneurysm (Aneu) with the turbulent flow by color Doppler (C). Both (B) and (C) are classic parasternal long-axis views with the LA posteriorly and to the left and the LV posteriorly and to the right. (D) This frame shows a peak Doppler flow velocity of 3.5 m/s with a calculated gradient of 49 mmHg. Reproduced from Ref.[52].

dimension. Coarctation of the aorta or interruption of the aortic arch may be present in approximately 30% of patients; these aortic obstructive lesions are observed only in patients with an unobstructed pulmonary outflow. PDA is present in almost 80% of cases.

Echo-Doppler studies are exceptionally helpful in making the diagnosis and in supplying adequate data for the development of management plans. The atretic atrial floor [Figures 72 and 73], whether it is due to an absent connection or imperforate membranous valve, is visualized in most cases, although such a distinction is not important in the management. It is also important to determine whether the defect is a part of complete AVSD, or if there is left AV valve atresia with a patent right AV valve; this determination is important because a complete AVSD is unlikely to produce left atrial obstruction (because of a usually large ostium primum ASD) while in mitral atresia with the hypoplastic left atrium, the inter-atrial communication can become obstructive [Figures 72B and 74] with time.

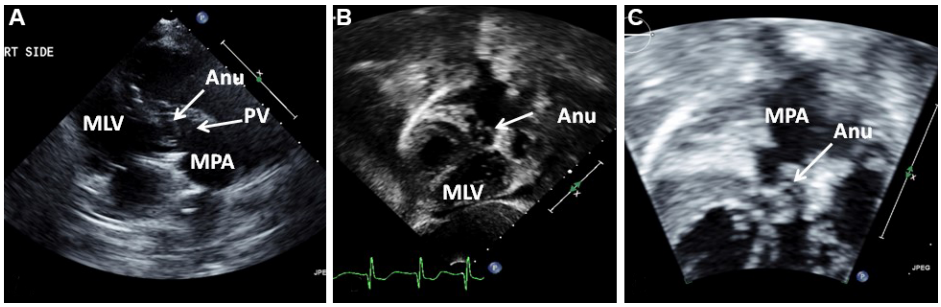

Figure 66. Selected video frames from right parasternal (A) and subcostal four-chamber (B) views of the morphological left ventricle (MLV) showing an aneurysm (Anu) protruding into the pulmonary outflow tract, causing an obstruction. The Anu is located just below the pulmonary valve (PV). A dilated main pulmonary artery (MPA) is also shown. (A) is a modified right parasternal view showing MLV to the left, PV in the middle with an Anu below the PV. (B) is a modified subcostal four-chamber view showing MLV to the right and Anu in the middle. (C) is a magnified view of (B), again illustrating the aneurysm and dilated MPA. Reproduced from Ref.[56].

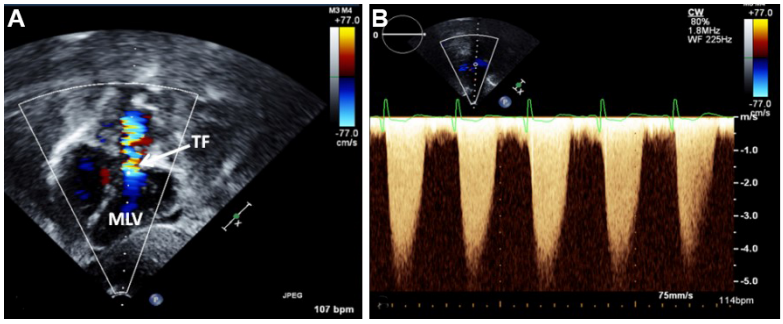

Figure 67. (A) Selected video frame from a subcostal four-chamber view (similar to Figure 66B) with color Doppler demonstrating turbulent flow (TF) in the pulmonary outflow tract. (B) Continuous wave Doppler recording across the pulmonary outflow tract demonstrates a peak Doppler velocity of approximately 5 m/s, suggesting significant obstruction. Reproduced from Ref.[56]. MLV: Morphological left ventricle.

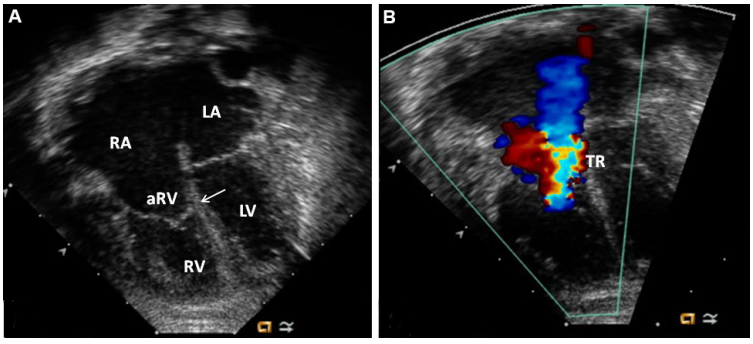

Figure 68. Apical four-chamber views of an echocardiogram of a baby with a mild to moderate form of Ebstein's anomaly. Panel (A) shows a two-dimensional image demonstrating the insertion of the septal leaflet of the tricuspid valve (arrow), which is displaced apically in comparison to the insertion of the mitral valve. The atrialized right ventricle (aRV) is shown. Panel (B) shows a color Doppler image demonstrating moderate tricuspid valve regurgitation (TR). Reproduced from Ref.[58]. LA: Left atrium; LV: left ventricle; RA: right atrium; RV: right ventricle.

The next step is to determine whether there is one ventricle (single ventricle) or two. In the latter case, the type of ventricular looping (d loop *vs.* l loop), the diameter of the VSD, and the origins of the aorta and PA should be defined. The pulmonary valve should be scrutinized to see if it is patent, stenosed or atretic and if there is stenosis, CW Doppler may evaluate the degree of obstruction. Suprasternal notch views should be

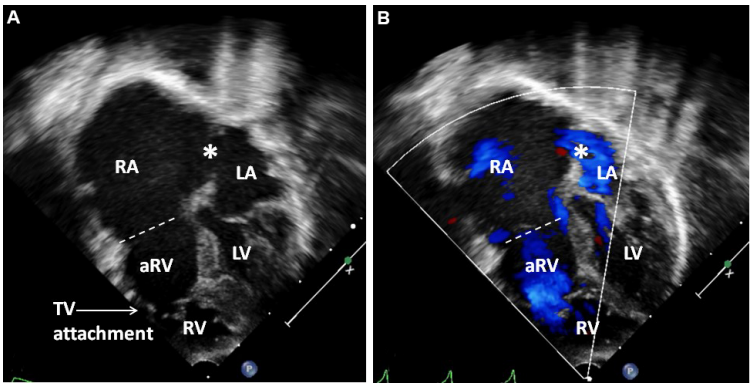

Figure 69. An echocardiogram of another baby with Ebstein's anomaly. Apical four-chamber views are shown. (A) Shows a two-dimensional image. (B) Shows the same image with color Doppler flow mapping. Note the significant downward displacement of the tricuspid valve (TV) attachment (solid arrow labeled "TV attachment") from the true annulus of the tricuspid valve (marked by a dotted line). The portion of the right ventricle (RV) between the tricuspid valve annulus and the tricuspid valve attachment is the atrialized portion of the right ventricle (aRV). *Represents the location of the patent foramen ovale. The color Doppler image in B shows right to left shunting (blue color). Note the markedly enlarged right atrium (RA) in both (A) and (B). Reproduced from Ref.[60]. LA: Left atrium; LV: left ventricle.

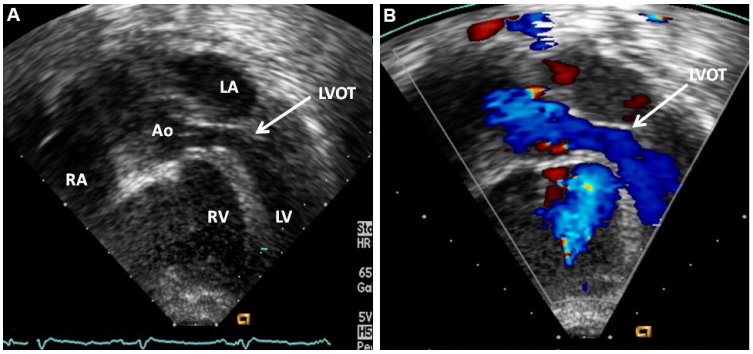

Figure 70. An apical five-chamber view of an echocardiogram showing a two-dimensional frame without (A) and with (B) color Doppler showing the bulging of the right ventricle (RV) into the left ventricular outflow tract (LVOT) in a patient with Ebstein's anomaly of the tricuspid valve. In this example, there is no significant obstruction; note the laminar flow in the LVOT and aorta (Ao). Reproduced from Ref.[58]. LA: Left atrium; LV: left ventricle; RA: right atrium.

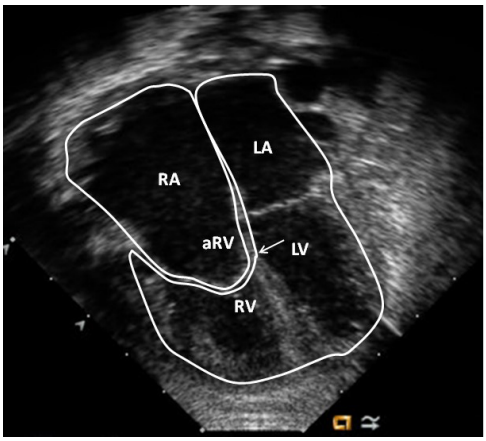

Figure 71. An apical four-chamber view showing all chambers of the heart in end-diastole. Tracing on the image shows the two areas used to obtain the ratio (Celermajer index) for prediction of outcome in fetal and neonatal echocardiograms (see text for further details). The abbreviations are the same as those used in [Figure 68]. Reproduced from Ref.[58].

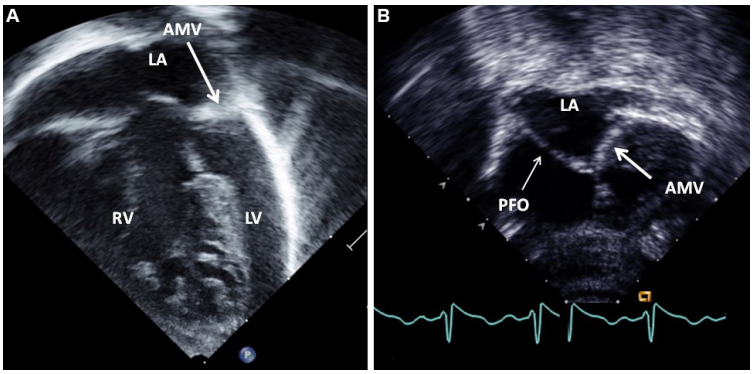

Figure 72. Selected video frames from modified apical four-chamber views of two infants (A, B) with mitral atresia, demonstrating atretic mitral valves (AMV), indicated by thick arrows in (A) and (B). A small left atrium (LA) and left ventricle (LV), and a large right ventricle (RV) are also seen. The thin arrow in (B) shows a restrictive patent foramen ovale (PFO). Reproduced from Ref.[39].

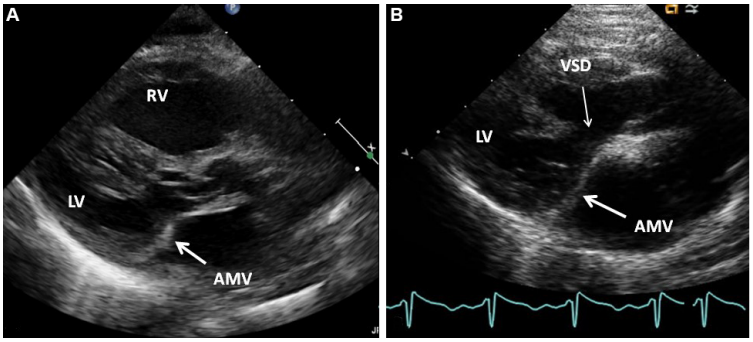

Figure 73. Selected video frames from parasternal long-axis views of two infants (A, B) with mitral atresia, demonstrating atretic mitral valves (AMV), indicated by thick arrows. In (B) a ventricular septal defect (VSD) is shown by a thin arrow. A small left ventricle (LV) and a large right ventricle (RV) are also seen, particularly in (A). Reproduced from Ref.[39].

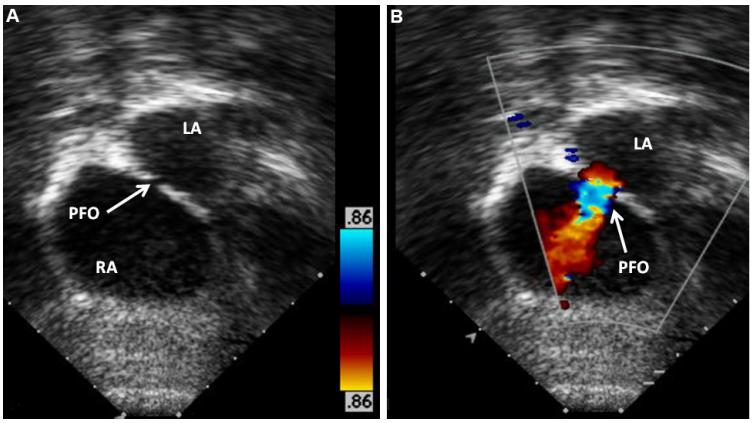

Figure 74. Selected video frames from subcostal echocardiographic views of an infant with mitral atresia, indicating a small and restrictive patent foramen ovale (PFO) (arrow in A). In (B), color flow mapping shows color acceleration (arrow in B) across this site. LA: Left atrium; RA: right atrium. Reproduced from Ref.[39].

examined along with Doppler interrogation to detect aortic coarctation or interruption. Cardiac catheterization with cine-angiography is rarely necessary for diagnosis; however, it is required in cases of restrictive ASD/PFO for performing catheter-based atrial septostomy[14,63].

SUMMARY AND CONCLUSIONS

In this paper, echo-Doppler findings of more frequently seen cyanotic CHDs were reviewed. At first, a brief description of the anatomic and pathophysiological features of each defect was presented; this is followed by detailing echocardiographic findings. The lesions discussed were TOF, TGA, tricuspid atresia, TAPVC, truncus arteriosus, HLHS, DORV, DILV, interrupted aortic arch, pulmonary atresia with IVS, congenital corrected TGA, Ebstein's anomaly of the tricuspid valve, and mitral atresia with normal aortic root. The pathologic features, ventricular function (see Part I) and hemodynamic abnormalities of cyanotic CHDs can be adequately evaluated by conventional echo-Doppler studies (m-mode, 2D and pulsed, CW and Color Doppler). In cases where this is not possible, other types of echocardiographic studies such as contrast echocardiography, trans-esophageal echocardiography, intracardiac echocardiography, intravascular ultrasound, 3-dimensional echocardiography, and others may be used. If necessary, more recent techniques of advanced imagining technology, namely, virtual reality and augmented reality may be utilized. The echo-Doppler features are sufficiently characteristic to make a diagnosis of each of the cyanotic CHD, to elucidate their pathophysiology, and to evaluate the need for surgical or transcatheter intervention so that the need for studies such as MRI, CT or cardiac catheterization with selective cineangiography is rare.

DECLARATIONS

Acknowledgments

A number of echocardiographic pictures have been used as figures in this paper; these echocardiograms were secured at multiple academic institutions, including the current institution (the Children's Memorial Hermann Hospital, Houston, Texas), that the author was privileged to work. I sincerely thank the sonographers at these institutions for their diligence in securing high-quality images.

Authors' contributions

The author contributed solely to the article.

Availability of data and materials

Not applicable.

Financial support and sponsorship

None.

Conflicts of interest

The author declared that there are no conflicts of interest.

Ethical approval and consent to participate

Not applicable.

Consent for publication

Not applicable.

Copyright

© The Author(s) 2022.

REFERENCES

1. Biliciler-Denktas G, Ozcelik N. Fetal echocardiography - Part I. In: Rao PS, Vidyasagar D, editors. A multidisciplinary approach to perinatal cardiology, Volume 1. New Castle upon Tyne: Cambridge Scholars Publishing; 2021. p. 60-98.
2. Ozcelik N, Agarwal AK, Gupta M. Fetal echocardiography - Part II - congenital heart defects and their management. In: Rao PS, Vidyasagar D, editors. A multidisciplinary approach to perinatal cardiology, Volume 1. New Castle upon Tyne: Cambridge Scholars

Publishing; 2021. p. 97-158.
3. Rao PS. Diagnosis and management of cyanotic congenital heart disease: part I. *Indian J Pediatr* 2009;76:57-70. DOI PubMed
4. Rao PS. Congenital heart defects - a review. In: Rao PS, editor. Congenital heart disease - selected aspects. Rijeka: InTech; 2012. p. 3-44.
5. Alapati S, Rao PS. Tetralogy of Fallot. In: Rao PS, Vidyasagar D, editors. A multidisciplinary approach to perinatal cardiology, Volume 2. New Castle upon Tyne: Cambridge Scholars Publishing; 2021. p. 203-46.
6. Alapati S, Rao PS. Tetralogy of Fallot in the neonate. *Neonatol Today* 2011;6:1-10.
7. Redington A. Tetralogy of Fallot and pulmonary atresia with ventricular septal defect. In: Moller JH, Hoffman JIE, Benson DW, Van HRE gf, Wren C, editors. Pediatric cardiovascular medicine. Hoboken: Wiley-Blackwell; 2012. p. 590-608.
8. Rao B, Anderson RC, Edwards JE. Anatomic variations in the tetralogy of Fallot. *Am Heart J* 1971;81:361-71. DOI
9. Need LR, Powell AJ, del Nido P, Geva T. Coronary echocardiography in tetralogy of Fallot: diagnostic accuracy, resource utilization and surgical implications over 13 years. *J Am Coll Cardiol* 2000;36:1371-7. DOI PubMed
10. Liao P, Edwards WD, Julsrud PR, Puga FJ, Danielson GK, Feldt RH. Pulmonary blood supply in patients with pulmonary atresia and ventricular septal defect. *J Am Coll Cardiol* 1985;6:1343-50. DOI PubMed
11. Rao PS, Lawrie GM. Absent pulmonary valve syndrome. Surgical correction with pulmonary arterioplasty. *Br Heart J* 1983;50:586-9. DOI PubMed PMC
12. Rao PS. Transposition of the great arteries in the neonate. *Congenital Cardiology Today* 2010;8:1-10.
13. Rao PS. Transposition of the great arteries. In: Rao PS, Vidyasagar D, editors. A multidisciplinary approach to perinatal cardiology, Volume 2. New Castle upon Tyne: Cambridge Scholars Publishing; 2021. p. 164-94.
14. Rao PS. Role of interventional cardiology in neonates: Part I. Non-surgical atrial septostomy. *Congenital Cardiol Today* 2007;5:1-12. DOI
15. Rao P. A unified classification for tricuspid atresia. *Am Heart J* 1980;99:799-804. DOI PubMed
16. Rao PS. Terminology: tricuspid atresia or univentricular heart? In: Rao PS, editor. Tricuspid Atresia. Mount Kisco: Futura Publishing Co; 1982. p. 3-6.
17. Rao PS. Demographic features of tricuspid atresia. In: Rao PS, editor. Tricuspid Atresia. Mount Kisco: Futura Publishing Co; 1992. p. 23-37.
18. Rao PS, Alapati S. Tricuspid atresia in the neonate. *Neonatology Today* 2012;7:1-12.
19. Rao PS. Echocardiographic evaluation of neonates with suspected heart disease. In: Rao PS, Vidyasagar D, editors. Perinatal cardiology: a multidisciplinary approach. Minneapolis: Cardiotext Publishing; 2015.
20. Rao PS. Tricuspid atresia. In: Rao PS, editor. Pediatric cardiology: how it has evolved over the last 50 years. New Castle upon Tyne: Cambridge Scholars Publishing; 2020. p. 24-69.
21. Rao PS. Echocardiographic evaluation of neonates with suspected heart disease. In. Rao PS, Vidyasagar D, editors. A multidisciplinary approach to perinatal cardiology, Volume 1. New Castle upon Tyne: Cambridge Scholars Publishing; 2021. p. 314-408.
22. Rao P. Diagnosis and management of cyanotic congenital heart disease: part II. *Indian J Pediatr* 2009;76:297-308. DOI PubMed
23. Whitfield CK, Rao PS. Total anomalous pulmonary venous connection in the neonate. *Neonatol Today* 2013;8:1-7.
24. Rao PS, Whitfield CK. Total anomalous pulmonary venous connection. In: Rao PS, Vidyasagar D, editors. A multidisciplinary approach to perinatal cardiology, Volume 2. New Castle upon Tyne: Cambridge Scholars Publishing; 2021. p. 294-312.
25. Craig JM, Darling RC, Rothney WB. Total pulmonary venous drainage into the right side of the heart; report of 17 autopsied cases not associated with other major cardiovascular anomalies. *Lab Invest* 1957;6:44-64. PubMed
26. Smith B, Frye TR, Newton WA, Jr. Total anomalous pulmonary venous return: diagnostic criteria and a new classification. *Am J Dis Child* 1961;101:41-51. DOI
27. Rao PS, Silbert DR. Superior vena caval obstruction in total anomalous pulmonary venous connexion. *Br Heart J* 1974;36:228-32. DOI PubMed PMC
28. Rao PS, Balaguru D. Truncus arteriosus in the neonate. *Neonatol Today* 2013;8:1-6.
29. Balaguru D, Rao PS. Truncus arteriosus. In: Vijayalakshmi IB, Rao PS, Chugh R, editors. A comprehensive approach to congenital heart diseases. New Delhi: Jaypee Brothers Med Publishers (P) Ltd.; 2013. p. 604-17.
30. Balaguru D, Rao PS. Truncus arteriosus. In: Rao PS, Vidyasagar D, editors. A multidisciplinary approach to perinatal cardiology, Volume 2. New Castle upon Tyne: Cambridge Scholars Publishing; 2021. p. 318-32.
31. Collett RW, Edwards JE. Persistent truncus arteriosus: a classification according to anatomic types. *Surg Clin North Am* 1949;29:1245-70. DOI PubMed
32. Noonan JA, Nadas AS. The hypoplastic left heart syndrome. *Pediat Clinics N Am* 1958;5:1029-56.
33. Rao PS, Striepe V, Merrill WM. Hypoplastic left heart syndrome. In: Kambam J, editor. Cardiac anesthesia for infants and children. St. Louis: Mosby; 1993. p. 299-309.
34. Rao PS, Turner R, Forbes TJ. Hypoplastic left heart syndrome. Available from: https://emedicine.medscape.com/article/890196-overview [Last accessed on 7 Apr 2022].
35. Alapati S, Rao PS. Hypoplastic left heart syndrome in the neonate. *Neonatol Today* 2011;6:1-9.
36. Rao PS, Alapati S. Hypoplastic left heart syndrome. In: Vijayalakshmi IB, Rao PS, Chugh R, editors. A comprehensive approach to management of congenital heart diseases. New Delhi: Jaypee Publications; 2013. p. 665-78.
37. Rao PS, Alapati S. Hypoplastic left heart syndrome. In: Rao PS, Vidyasagar D, editors. A multidisciplinary approach to perinatal

cardiology, Volume 2. New Castle upon Tyne: Cambridge Scholars Publishing; 2021. p. 335-72.
38. Buck SH, Rao PS, Merrill W, Kambam J. Double-outlet right ventricle. In: Kambam J, editor. Cardiac anesthesia for infants and children. St. Louis: Mosby; 1993. p. 312-39.
39. Rao PS. Other cyanotic heart defects in the neonate. In: Rao PS, Vidyasagar D, editors. A multidisciplinary approach to perinatal cardiology, Volume 2. New Castle upon Tyne: Cambridge Scholars Publishing; 2021. p. 474-509.
40. Rao PS, Sissman NJ. Spontaneous closure of physiologically advantageous ventricular septal defects. *Circulation* 1971;43:83-90. DOI PubMed
41. Rao P. Left ventricular obstruction in double outlet right ventricle. *Am Heart J* 1972;83:289-90. DOI PubMed
42. Rao PS. Physiologically advantageous ventricular septal defects. *Pediatr Cardiol* 1983;4:59-61. DOI PubMed
43. Rao P. Subaortic obstruction after pulmonary artery banding in patients with tricuspid atresia and double-inlet left ventricle and ventriculoarterial discordance. *J Am Coll Cardiol* 1991;18:1585-6. DOI PubMed
44. Sharma SK, Rao PS. Interrupted Aortic Arch. The encyclopedic reference of molecular mechanisms of disease. Berlin: Springer-Verlag; 2008.
45. Celoria GC, Patton RB. Congenital absence of the aortic arch. *Am Heart J* 1959;58:407-13. DOI PubMed
46. Kaulitz R, Jonas RA, van der Velde ME. Echocardiographic assessment of interrupted aortic arch. *Cardiol Young* 1999;9:562-71. DOI PubMed
47. Rao PS. Comprehensive management of pulmonary atresia with intact ventricular septum. *Ann Thorac Surg* 1985;40:409-13. DOI PubMed
48. Siblini G, Rao PS, Singh GK, Tinker K, Balfour IC. Transcatheter management of neonates with pulmonary atresia and intact ventricular septum. *Cathet Cardiovasc Diagn* 1997;42:395-402. DOI PubMed
49. Rao PS. Pulmonary atresia with intact ventricular septum. *Curr Treat Options Cardiovasc Med* 2002;4:321-36. DOI PubMed
50. Balaguru D, Rao PS. Pulmonary atresia with intact ventricular septum. In: Rao PS, Vidyasagar D, editors. A multidisciplinary approach to perinatal cardiology, Volume 2. New Castle upon Tyne: Cambridge Scholars Publishing; 2021. p. 381-403.
51. Rao PS. Other tricuspid valve anomalies. In: Long WA, editor. Fetal and Neonatal Cardiology. Philadelphia: W.B. Saunders Company; 1990. p. 541-50.
52. Reddy SB, Chopra PS, Rao P. Aneurysm of the membranous ventricular septum resulting in pulmonary outflow tract obstruction in congenitally corrected transposition of the great arteries. *Am Heart J* 1997;133:112-9. DOI PubMed
53. Wallis GA, Debich-Spicer D, Anderson RH. Congenitally corrected transposition. *Orphanet J Rare Dis* 2011;6:22. DOI PubMed PMC
54. Ferencz C, Rubin JD, McCarter RJ, et al. Congenital heart disease: prevalence at livebirth. The Baltimore-Washington Infant Study. *Am J Epidemiol* 1985;121:31-6. DOI PubMed
55. Rogers JH Jr, Rao PS. Ebstein's anomaly of the left atrioventricular valve with congenital corrected transposition of the great arteries. Diagnosis by intracavitary electrocardiography. *Chest* 1977;72:253-6. DOI PubMed
56. Yarrabolu TR, Thapar MK, Rao PS. Subpulmonary obstruction due to aneurysmal ventricular septum in a patient with congenitally corrected transposition of the great arteries and dextrocardia. *Congenital Cardiology Today* 2014;12:1-8. DOI
57. Rao PS, Kambam J. Ebstein's malformation of the tricuspid valve. In: Kambam J, editor. Cardiac anesthesia for infants and children. St. Louis: Mosby-Year Book; 1994. p. 320-32.
58. Balaguru D, Rao PS. Disease of the tricuspid valve. In: Vijayalakshmi IB, Rao PS, Chugh R, editors. A comprehensive approach to congenital heart diseases. New Delhi: Ed. Jaypee Brothers Medical Publishers; 2013. p. 414-33.
59. Balaguru D, Rao PS. Ebstein's anomaly of the tricuspid valve in the neonate. *Neonatol Today* 2015;10:1-6.
60. Balaguru D, Rao PS. Ebstein's malformation of the tricuspid valve. In: Rao PS, Vidyasagar D, editors. A multidisciplinary approach to perinatal cardiology, Volume 2. New Castle upon Tyne: Cambridge Scholars Publishing; 2021. p. 408-28.
61. Celermajer DS, Cullen S, Sullivan ID, Spiegelhalter DJ, Wyse RK, Deanfield JE. Outcome in neonates with Ebstein's anomaly. *J Am Coll Cardiol* 1992;19:1041-6. DOI PubMed
62. Andrews RE, Tibby SM, Sharland GK, Simpson JM. Prediction of outcome of tricuspid valve malformations diagnosed during fetal life. *Am J Cardiol* 2008;101:1046-50. DOI PubMed
63. Balaguru D, Rao PS. Mitral Atresia (With Normal Aortic Root). In: Vijayalakshmi IB, Rao PS, Chugh R, editors. A comprehensive approach to management of congenital heart diseases. New Delhi: Jaypee Publications; 2013. p. 458-67.